Silica-based organic–inorganic hybrid nanomaterials for optical bioimaging

Ivana Miletto, Enrica Gianotti, Marie-Hélène Delville, Gloria Berlier

17. Silica-based Organic-Inorganic Hybrid Nanomaterials for Optical Bioimaging

Ivana Miletto,[1] Enrica Gianotti,[1] Marie-Hélène Delville,[2] Gloria Berlier[3]

[1] Università del Piemonte Orientale, Dipartimento di Scienze ed Innovazione Tecnologica, Viale Teresa Michel 11, Alessandria, 15100, Italy

[2] CNRS, Université de Bordeaux, Institut de Chimie de la Matière Condensée de Bordeaux (ICMCB), 87 avenue du Dr. A. Schweitzer, Pessac, F-33608, France.

[3] Università di Torino, Department of Chemistry and NIS Centre (Nanostructured Surfaces and Interfaces), Via P. Giuria 7, Torino, 10125, Italy

ABSTRACT

Starting from the general definition of hybrid nanomaterials, the introductory section will draw the readers' attention to the main issues concerning the use of fluorescent probes for in vitro and in vivo bioimaging and the general requirements for "the optimal probe". The benefits arising from the use of hybrid materials will be outlined especially concerning: 1 Non porous Fluorescent Silica nanoparticles. 2 Mesoporous silica based nanoparticles and Fluorescent Organosilicas. 3 Zeolites. In this section the recent advances in the preparation and characterization of nanosized zeolite crystals will be reviewed; different strategies of incorporation of fluorescent compound will be considered.

KEY WORDS

Silica nanoparticles, fluorescence, Mesoporous materials

17.1. Introduction to hybrid nanomaterials for bioimaging

Hybrid organic–inorganic nanomaterials are not simply physical mixtures but are considered and defined as the result of their intentional combination, using soft inorganic chemistry, of organic and inorganic units at molecular/nanoscale level, thereby opening access to a wide spectrum of multifunctionality not possible with the traditional concepts of materials science. The nanostructure, degree of organization and properties of such materials do not only depend on the chemical nature and the synergies between their nano-units, but also strongly rely on the interface they share. The properties of such hybrid nanomaterials are not only the sum of the individual contributions of each phase, but also can also result from the role of their interface which can then become predominant. Since the review by Sanchez et Al. (1) the nature of the interface is used to sort these materials into two distinct classes. Class I refers to the hybrid materials where organic and inorganic components exhibit weak interactions where only hydrogen, van der Waals or ionic bonds give cohesion to the structure. In Class II materials, the two phases are linked together through strong covalent or iono-covalent chemical bonds. Chemists have so far designed, elaborated and processed many functional hybrid materials with enhanced properties by using soft chemistry routes based on the polymerization of functional organosilanes, macromonomers and metal alkoxides. They also used (i) the encapsulation of organic components within sol–gel derived organosilica or hybrid metal oxides (ii) the organic functionalization of nanofillers, nanoclays or other compounds with lamellar structures; (iii) the self-assembly or templated growth, (iv) nano-building block approaches, (v) hydrothermally processed hybrid zeolites or microporous metal organic frameworks, (vi) integrative synthesis or coupled processes, and (vii) bio-inspired strategies.(2) (3) (4) (5) (6) (7) These innovative organic–inorganic hybrid nanomaterials have major impacts in many application domains such as optics, electronics, mechanics, energy, environment, protective coatings, and more specifically biology, bio-imaging and medicine, the topics of this chapter.

Bio-imaging and clinical imaging modalities include complementary techniques (8) such as: optical imaging, (9-17) magnetic resonance imaging (MRI), (18-21) computed tomography (CT), (22) ultrasound imaging (USI) (23-27) positron emission tomography (PET) (28-31) and single photon emission computed tomography (SPECT) (32-34). Other techniques are also examined, for example multi-photon plasmon resonance microscopy, (35) optical coherence tomography (OCT), (36) surface enhanced Raman spectroscopy (SERS), (9, 37-41) as well as diffuse optical spectroscopy (42). Some techniques enable an entire-organism anatomical imaging (e.g. MRI or PET) while others provide more specific molecular imaging (*e.g.*, optical fluorescence or USI) at the subcellular resolution. Combination of these different tools is aimed at a better diagnosis of early-stage cancer,

guided stem cell therapies, drug delivery, pathogen detection, gene therapy, image-guided surgery, and cancer staging. (43)

Among all these techniques used for bio-imaging (44) the fluorescence bio- imaging one is essential in pre-clinical investigations, and the research of suitable and accurate tools for *in vivo* measurements is becoming crucial and raising more and more attention. The use of nanotechnology allowed solving the encountered limitations, and luminescent nanoparticles (NPs) are one of the most promising materials proposed for future diagnostic implementation and breakthrough. NPs constitute also a versatile nanohybrid platform that can allow facile multiple functionalization to perform multimodal imaging or theranostic (simultaneous diagnosis and therapy).

To help improving these techniques resolution, nanohybrid particles have proved as very powerful probes for both *in vivo* imaging in medical and *in vitro* biological diagnostics. Several types of NPs have been used to generate breakthroughs as compared to common molecular probes improving their properties and detection limits, in a broad array of imaging modalities. The specifications of an ideal probe are numerous. It should exhibit colloidal stability in *in vivo* biological media, non-dependence on the solvent polarity, ionic strength, pH, or temperature. Other properties such as limited nonspecific binding, resistance to the reticulo-endothelial system (RES) uptake, and easy natural clearance are also required. High sensitivity, good contrast quality (high signal-to-noise ratio, (SNR)) and long enough blood circulation periods are also compulsory. In other words, this NP should have the adapted long-term quantitative imaging at low doses and be safely cleared from the body after imaging completion.

Among these nanohybrid platforms this chapter will more specifically focus on silica-based luminescent hybrid nanoparticles which exhibit a very rich chemistry and therefore offer very appealing approaches. For example, compared to Magnetic Resonance Imaging, optical imaging is much easier to use, cost-effective, and can be applied to cancer diagnosis with high resolution.(39) (45) NIR dye-doped silica NPs are becoming more and more popular as contrast agents for several recognized reasons: silica NPs as detailed below, are optically transparent, water dispersible, biologically inert, nontoxic in the amorphous form, with well-established conjugation strategies to modify the surface with proteins, peptides, and other ligands for cellular receptors using the well-known silane chemistry. The use of such a matrix, in which many NIR fluorophores can be encapsulated, reduces the potential toxicity of these fluorescent probes and shields the NIR emitter from the aqueous environment, where the dye usually suffers from low fluorescence quantum yield, degradation, and unsatisfactory photostability. NIR-emitting dyes such as polymethines (Cy5.5, Cy7), indocyanine green (ICG), Alexa Fluor 750, and IRDye78 have already been incorporated into silica NPs. Encapsulation of multiple dyes within a single silica NP generates much brighter and

more stable probes than those loaded with a single one. Dye-doped silica NPs are usually synthesized by a sol–gel Stöber process or in microemulsion by simply adding the dye (or a modified form of the dye) to the silica-forming solution.(46) In addition, the use of mesoporous silica NPs enables the loading of an additional functions into the resulting pores, for example imaging probes of sentinel lymph nodes (SLNs) known as the first defense against primary tumor metastasis, (47) sensing (48) or a therapeutic agent capable of photothermal ablation or a controlled drug release (49). The covalent chemical grafting of lanthanide complexes on metal oxide nanoparticles was also recently performed and introduction of two different lanthanides gave bimodal contrast agents (50-52).

17.2. Fluorescent Silica nanoparticles

Among the wide variety of hybrid nanomaterials developed for bioimaging purposes, fluorescent silica nanoparticles (SiNPs) prepared by encapsulation and/or grafting of luminescent moieties (e.g. fluorescent organic and organometallic dyes, luminescent lanthanides, metallic nanoparticles and quantum dots)(53-55) in the silica framework represent one of the most versatile and exploited families (56), being capable of offering all the required features to obtain effective tools for diagnostic and theranostic applications (57-59). Silica itself exhibits a wide variety of attractive characteristics that can be beneficial when designing a nanosized probe (60); first of all, SiNPs possess a well-known and tunable surface chemistry. As a consequence, the surface of SiNPs can be easily functionalized using conventional silane-based chemistry (56, 61, 62) in order to improve colloidal stability, biocompatibility, cell-permeation properties, to tune the circulation time and clearance, as well as to introduce functional groups exploitable to conjugate biomolecules for specific targeting (e.g. monoclonal antibodies, nucleic acids, small ligands, etc..). Second, silica matrix is optically transparent, that allows excitation and emission light to efficiently pass through the silica matrix. Third, amorphous silica appears to be resistant to swelling, biocompatible, non-toxic and easily excreted (depending on the size). Beside all these features, SiNPs has several advantages over other luminescent probes; extensive literature on the beneficial effects has been published in the last decade, including reports about increased photostability, quantum yield and brightness of organic and organometallic fluorophores upon encapsulation in SiNPs, as well as gained water solubility and efficient conjugation.

Given the vast diversity of fluorescent molecules and their exquisite sensitivity to their local environment, the encapsulation in SiNPs raises the possibility of developing systems with a broad

range of precisely controlled luminescence characteristics (63) which can be exploited in fluorescence detection. The term fluorescence does not imply a single spectroscopic method but rather includes a variety of techniques in which imaging can be obtained by measuring signal intensity, decay time, polarization, and also by studying effects caused by fluorescence resonance energy transfer (FRET), up-conversion, quenching, or photo-induced electron transfer (64).

Therefore, the fluorescence properties of different nanotools should be tailored on the basis of the desired effect; as for example, in the case of SiNPs to be used as imaging probe for signal intensity-based techniques the overall quantum yields and brightness should be maximized and aggregation phenomena, which often lead to fluorescence quenching, should be avoided. On the contrary, when dealing with FRET-based techniques the SiNPs should be engineered in order to ensure optimal proximity of FRET pairs (65).

In this section, examples of SiNPs engineered in order to fulfil different requirements will be reviewed, highlighting that SiNPs architecture determines radiative properties of encapsulated fluorophores.

17.2.1. Non-covalent entrapment of fluorophores

Fluorescent SiNPs can be obtained using sol-gel processes under various conditions that give rise to different final materials through the fine tuning of various parameters such as catalytic conditions, nanoparticles nucleation and growth confinement (57). The main preparation approaches are the Stöber-Van Blaaderen method (66) and the methods involving hydrolysis and condensation confinement, such as the reverse microemulsion method (67) and direct micelle assisted method (68). Irrespective of the preparation method and of the fluorescent moiety employed, the performance of the final nanomaterial is determined to a significant extent by the distribution of the photoluminescent molecules within the host matrix because intermolecular interactions can occur modifying the photophysical properties (69).

Seminal works by Santra and co-workers (62, 70) reported that the fluorophore can be simply added as such to be entrapped into the growing silica matrix. In particular, they synthesized fluorescent SiNP doped with Tris(2, 28-bipyridyl)dichlororuthenium (II) hexahydrate (Rubpy) by following the reverse microemulsion approach and adding the fluorophore dissolved in the water pool of the microemulsion. The authors did not observe any leaking of Rubpy dye from the SiNP, maybe due to a successful complete encapsulation of the dye into the silica matrix and due to weak interactions between the silica oxygen atom and the ruthenium ion, which can be also responsible for the red-shift observed in the emission spectra of the SiNP, when compared to the pure dye in the solid state.

In order to optimize the performance of the SiNP, the authors investigated different Rubpy loading, demonstrating that self-quenching occurs above a certain Rubpy concentration. The protective role of the silica matrix towards the photo-oxidation of the fluorescent guest was confirmed with photobleaching experiments and pressure dependent emission studies, indicating that the dye molecules are protected from the surrounding environment and that the silica matrix is impermeable for oxygen under normal air pressure. Although direct incorporation within the water pool of the microemulsion, as well as the effective incorporation in SiNPs prepared with the Stöber method, is working well with hydrophilic dyes, several efforts have been done to promote the incorporation of hydrophobic dyes which cannot be dissolved in water droplets. To address this problem, hydrophobic dyes, such as Tetramethylrhodamine (TMR), were converted to hydrophilic molecules by linking a dextran molecule to TMR. Keeping the TMR-dextran inside the silica matrix was achieved by making water droplets acidic; with these modifications, uniform and highly fluorescent SiNPs were synthesized, without leakage of the fluorophore (71). This approach was further followed for the incorporation of fluorescein molecules into SiNPs (72), whilst a different approach was proposed by Tapec and co-workers (73) who used a combination of two silica precursors, tetraethylorthosilicate and phenyltriethoxysilane, to synthesize SiNPs-doped with hydrophobic dyes. They demonstrated that the hydrophobic nature of phenyltriethoxysilane helps keeping the organic dye in the silica matrix, whereas the hydrophilic tetraethylorthosilicate-formed silica allows the resulting nanoparticles to be dispersed in aqueous solutions. Characterization of the so-obtained SiNPs showed that they could be synthesized in the nanometer range with high photostability and minimal dye leakage.

17.2.2. Covalent immobilization of alkoxysilane-derivatized fluorophores

The first examples of the use of alkoxysilane-derivatized fluorophores for the stable doping of SiNPs was reported by Van Blaaderen and co-workers (74), who prepared fluorescent SiNPs with the Stöber method by using a fluorescein isothiocyanate-aminopropyltriethoxysilane (FITC-APTS) derivative as fluorescent moiety. The authors demonstrated that it is possible to tune the distribution of the fluorophore in the silica matrix and, then, to have a good control on the photophysical properties of the system, simply by modifying the reaction procedure and alternating steps of FITC-APTS and silica precursors addition (Figure 17.1). Since then, a huge volume of literature has been published about the confinement of fluorescent dyes within SiNPs through either (i) the

derivatization of the fluorophore with alkoxysilane moieties and subsequent covalent bound to the growing silica matrix (75-77) or (ii) the chemical functionalization of the silica NPs by a commercial functional silane (78), followed by a further chemical coupling with the fluorescent agent. This fluorescent agent can be either an organic dye (79) or a rare earth complex (50, 80, 81).

Wiesner's group developed highly bright core-shell SiNPs embedding TRITC-APTS moieties where the TRITC-rich fluorescent core is surrounded by a silica shell (82). The same approach was later on applied for the preparation of fluorescent SiNPs with tunable color, thus covalently incorporating various fluorophores, such as AlexaFluor 350, N-(7-dimethylamino-4-methylcoumarin-3-yl)maleimide, AlexaFluor 488, fluorescein isothiocyanate, AlexaFluor 555, AlexaFluor 568, Texas Red, AlexaFluor 680 and AlexaFluor 750 (83), thus obtaining a wide variety of ultrasmall fluorescent SiNPs, called CU Dots (Cornell Dots) which have been tested in the first-in-human clinical trial in patients with metastatic melanoma for the imaging of cancer (84). Irrespective of the fluorescent dye used, the authors found that the brightness of the core was usually actually less than that of free dye, suggesting that the dense dye-rich core was heavily quenched compared to the free dye. However, upon addition of an outer, dye-free silica shell to the core, the brightness was increases by a factor of at least 30.

Similarly, Rampazzo et al. (85) demonstrated the spontaneous accumulation of dye molecules in the core of SiNPs. Pyrene was chosen because its fluorescence properties (quantum yield and fluorescence lifetime) are highly affected by quenching by molecular oxygen, furthermore pyrene molecules tend to form excimers at high concentration. Both features were exploited in order to monitor the dispersion of the dye into the silica matrix and to highlight its beneficial shielding effect towards to photooxidation and quenching. A strong enhancement of pyrene fluorescence and a corresponding increase of its excited-state lifetime was observed upon its inclusion, as a result of the shielding effect from molecular oxygen due to the silica matrix. Furthermore, in the case of high loading a heavily doped core showing an excimer-like emission is first formed. Further growth leads to the formation of layers where the concentration of pyrene gradually decreases and the monomeric emission becomes relevant (Figure 17-1).

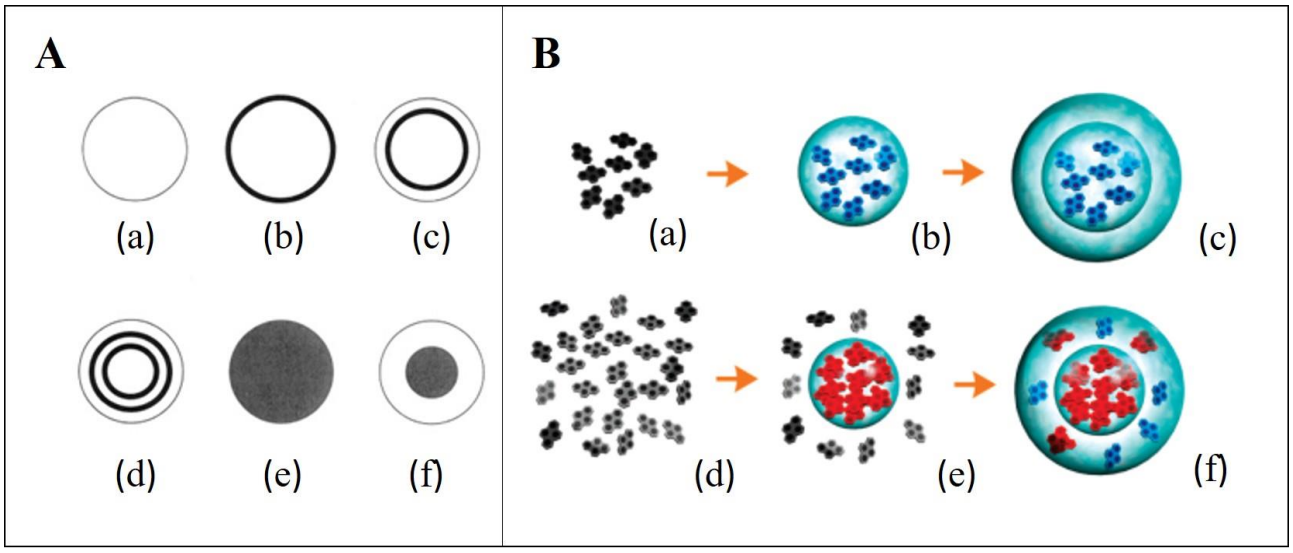

Figure 17 - 1. Schematic representation of the different ways FITC-APTS is distributed through the SiNP matrix. (a-f). The dark region stands for FITC-APTS-modified areas and white means "ordinary" silica. (Reprinted with permission from ref (74). Copyright 1992 American Chemical Society). B. Pictorial representation of the growing of SiNPs doped with pyrene-alkoxysilane derivatives (Reprinted with permission from ref. (85). Copyright 2007 American Chemical Society).

Another interesting example of manipulation of the photophysical properties of dye molecules upon encapsulation within nanometric SiNPs was proposed by Larson et al. (63); the control of the photophysical properties was accomplished through changes in silica architecture on the nanometer size scale and results in enhanced fluorescence quantum efficiency. The authors prepared a rhodamine-alkoxysilane precursor by reacting tetramethylrhodamine isothiocyanate (TRITC) with APTS and they used the resulting adduct as the fluorescent precursor for the preparation of core-shell SiNPs characterized by different architectures. Three architectural variations on the basic core-shell morphology were developed in order to achieve the desired enhancement/maximization of the fluorescence properties. These three architectures were (i) a compact core of dye surrounded by a silica shell, (ii) an expanded core containing the dye surrounded by a silica shell and (iii) a homogenous particle where the dye is homogeneously distributed within the silica matrix. All three systems were characterized by approximately the same size and composition, but the constituent dyes exhibited different photophysical properties. By optimizing the nanoparticle structure the authors achieved greater than 3-fold increase in the quantum efficiency of TRITC, mainly due to the reduction of non-radiative rates; such a reduction is related to the restricted rotational mobility of the fluorophore covalently bound within the particles: the more restricted is the mobility, the smaller the non-radiative rate.

Much higher quantum yield enhancement was obtained when an alkoxy-modified trimethine indocyanine dye was employed in the preparation of SiNPs via the reverse microemulsion method (86, 87). The combination of steady-state and time-resolved fluorescence revealed that almost all the fluorophore molecules exhibited the same photophysical behavior, suggesting that they should be dispersed in a monomeric form within the silica matrix. This results in a significant brightness enhancement and in an increased photostability with respect to the fluorophore in solution. The so obtained fluorescent SiNPs were tested as imaging probes in *in vitro* tests in highly differentiated neuronal cells (GT1-7), showing that the prepared nanoparticles can be incorporated with no apparent toxicity. Interestingly, the trimethine indocyanine dye used was not significantly soluble in water, which is apparently in contrast with the general idea that the microemulsion method could be more effective for the encapsulation of hydrophilic molecules (88). Indeed, it has to be noted that reverse microemulsion is a multiphasic system where the surfactant "palisade", along with the co-surfactant, is separating the water pool from the bulk oil phase. As a consequence, the partition of the molecular species involved in the formation of fluorescence SiNPs among the different phases of the microemulsion system can play a fundamental role in the final architecture of the hybrid material. In order to investigate the role of hydrophilicity/hydrophobicity of a fluorophore in determining its dispersion in SiNPs prepared in reverse microemulsion, Alberto et al. (69) carried out a systematic study based on the preparation of fluorescent SiNPs by the incorporation of three indocyanine-APTS derivatives differing only in the number of sulfonic groups and, hence, in their hydrophilicity (Figure 17.2). The goal of the research was the identification of molecular parameters that could effectively help tailoring the photophysical properties of the hybrid SiNPs. The evolution of the photophysical properties of the three indocyanine dyes was followed by means of spectroscopic techniques (UV-Vis absorption spectroscopy, steady-state and time-resolved photoluminescence) from the starting microemulsion to the final nanoparticles, providing evidence of the key role of the hydrophilicity of the fluorophore in ruling the dispersion within the silica matrix. In particular, hydrophilic indocyanine molecules (namely I3BS) were found to be present in the water pool from the early stages of the reaction, resulting in the heavy formation of non-luminescent aggregates within the silica matrix (Figure 17-2).

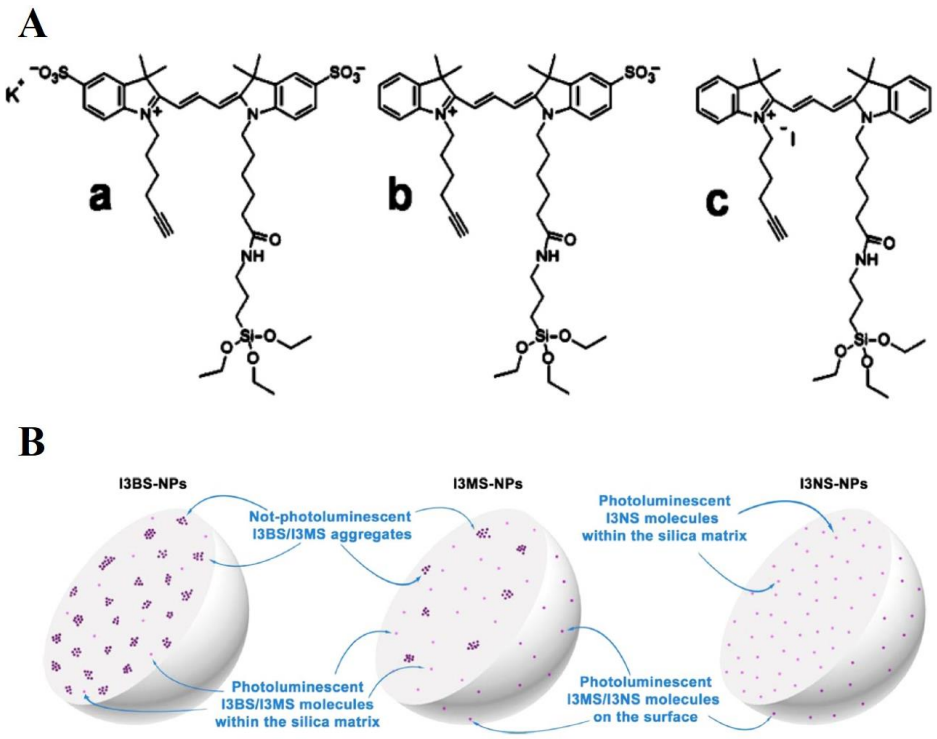

Figure 17 - 2. A. Structure of the three indocyanine dyes used by Alberto et al. B. Pictorial representation of the distribution of the indocyanine dyes within the final fluorescent SiNPs (Adapted with permission from ref. (69). Copyright 2012 American Chemical Society)

The indocyanine molecules characterized by an intermediate hydrophilicity value (namely I3MS) are preferentially located in an environment characterized by an intermediate polarity with respect to water and n-hexanol, present as a co-surfactant that is at the interface between the water pool and the inner side of the surfactant layer. As a consequence, in this case the formation of non-luminescent aggregates is somewhat reduced and a fraction of the luminescent molecules are located on the eternal surface of the SiNPs. Finally, I3NS molecules, due to their lower hydrophilicity, at the early stages of the reaction should be preferentially located near the outer side of the surfactant palisade, toward the oil phase. This induces a slow migration of the fluorophores in the water pool where the silica phase is growing, as soon as the trimethoxysilane moieties are hydrolyzed. As a consequence, I3NS molecules were found to be homogenously distributed both within the silica matrix and on the external surface, without evidence of non-luminescent aggregates formation.

Although most of the efforts widely reviewed in literature are devoted to the enhancement of luminescence properties through inhibition of aggregation of the fluorophores, recently, increasing attention has been focused on a new class of fluorophores which behavior upon aggregation is the opposite of traditional organic fluorophores (89), the so-called Aggregation-induced emission (AIE) fluorophores. AIE fluorophores are non-emissive in dilute solutions and are induced to emit intense

fluorescence upon aggregation; their confinement within nanosystems of different architecture and composition is emerging as a powerful technique for the control and enhancement of aggregation properties of AIE fluorophores (90, 91). This aggregation-enhanced effect offers an opportunity to produce a novel kind of dye-concentrated nanoparticles, where dye-aggregation is not detrimental but rather enhances fluorescence efficiency. In contrast to nanoparticles encapsulating common fluorophores, one can expect that the fluorescence output from such nanoparticles can be increased readily by raising the loading, because the interdependency between fluorescence efficiency and loading density is no more governed by concentration quenching. Several examples are present in literature about AIE fluorophores both embedded and covalently bound to SiNPs, which is not possible to exhaustively review here. Kim et al (92) developed an anthracene derivative which has been shown to enhance one- and two-photon fluorescence without any intermolecular quenching effect, which enabled remarkable signal improvement by raising its loading density in the composite nanoparticles. The so obtained nanosystems were successfully applied in in vitro experiments, highlighting they are promising candidates as two-photon fluorescence probes for biomedical applications. Furthermore, energy-transferring organically modified silica nanoparticles for two-photon photodynamic therapy (PDT) were developed (93) by co-encapsulating two-photon fluorescent dye nanoaggregates as an energy up-converting donor and a photosensitizing drug for PDT as an acceptor. The authors successfully combined the aggregation-enhanced two-photon absorption and emission properties of the AIE fluorophore and the nanoscopic FRET between the aggregated AIE fluorophore and the photosensitizer; the preliminary in vitro tests showed that singlet oxygen generation in cancer cells by photosensitization can be observed under two-photon irradiation. In order to avoid dye leakage, Faisal and coworkers (94) proposed a surfactant-free sol-gel process to obtain core-shell structures where the AIE fluorophore was chemically bound to, rather than simply embedded within, the forming silica networks. The resultant SiNPs were mono-dispersed, with smooth surface, high surface charge and excellent colloidal stability and emission intensities could be tunable by changing the reaction conditions and the fluorophore loading. Another example of successful covalent immobilization of AIE fluorophores in SiNPs was proposed by Mahtab *et al.* (95) who reported about the fabrication of fluorescent SiNPs with efficient light emission, colloidal stability and size tenability by one-pot, two-step Stöber and reverse microemulsion methods. Tetraphenylethene (TPE) and silole[1] functionalized siloxanes were

[1] Siloles, also called silacyclopentadienes, are the silicon analogs of cyclopentadienes.

prepared by click reactions and used along with the precursor TEOS to generate fluorescent SiNPs. UV irradiation of the so obtained nanosystems results in strong blue and green light, thanks to the novel aggregation-induced emission features of the TPE and silole aggregates in the hybrid nanoparticles.

Another field of application where fluorophore should not be homogeneously dispersed in a silica matrix as isolated molecules is the design of fluorescence probes for FRET-based imaging techniques. FRET is a process in which energy is transferred from an excited donor to an acceptor molecule, leading to a reduction in the donor's fluorescence emission and an increase in the acceptor's fluorescence emission intensities. Since the energy transfer efficiency is distance dependent, it can only occur over distances smaller than a critical radius, known as the Förster radius (65). Although the most efficient silica nanosystems for the hosting of FRET systems are mainly represented by mesoporous systems where the dyes can be arranged in an ordered fashion, some interesting examples of non-porous SiNPs engineered for FRET applications should be reviewed. Wang and Tan reported the preparation of multicolor FRET SiNPs (96); triple-dye-doped FRET SiNPs were prepared via a Stöber modified method. The three tandem dyes were carefully chosen in order to allow an efficient FRET. FITC, Rhodamine 6G (R6G), and carboxy-rhodamine (ROX) were selected because of their good spectral overlapping, which is one of the requirements for and effective FRET pairing. In the triple-dye-doped NPs, FITC was used as a common donor for R6G and ROX, while R6G acted as both an acceptor for FITC and a donor for ROX. Slight variations in the doping ratio of the three tandem dyes results in fine tuning of the FRET-mediated emission and the different SiNPs exhibit different colors under one single wavelength excitation, as reported in Figure 17.3.

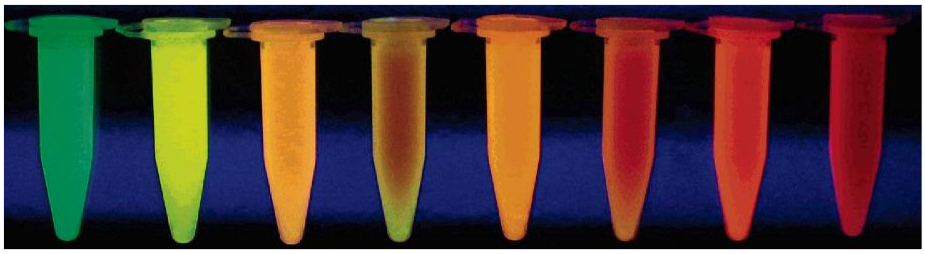

Figure 17 - 3 FRET-SiNP samples with different doping dye combinations under 300-nm UV illumination. Dye doping ratio (from left to right) FITC:R6G:ROX = 1:0:0, 0:1:0,1:0:1, 4:1.5:3, 0.5:0.5:0.5, 2:2:2, 0:1:1, 0.5:0.5:4. (Reprinted with permission from ref. (96) . Copyright 2006 American Chemical Society)

Using a similar strategy, Xu and coworkers (97) developed two-dyes doped FRET SiNPs by incorporating two dyes, fluorescein isothiocyanate, FITC, as the donor and an organometallic complex (tris(1,10-phenanthroline) ruthenium, $Ru(phen)_3^{2+}$) as the phosphorescent acceptor. In

order to investigate the effect of dyes distribution and donor-acceptor distance on the photoemission properties of the resulting SiNPs, the two dyes were incorporated within the silica nanoparticles by two different strategies, step-wise doping and co-doping. The latter consists in the incorporation of the two dyes into the same silica layer, whilst in the stepwise doping the two dyes were incorporated in successive layers, separated from each other by a silica layer of variable thickness (from 2 to 12 nm). Final colour of the nanoparticles resulted to be tuneable by changing both the ration between donor and acceptor doping rate, and by changing the doping strategy.

The ability to control the photophysical properties through nanoparticles architecture enables both the development of next generation of fluorescent probes and the tailoring of their properties in order to fulfil the particular requirements related to each particular application; in addition, further engineering of silica surface allows the incorporation of several functionalities within the same nanoparticle, which is the starting point for the development of effective multifunctional smart materials.

17.3. Mesoporous silica based nanoparticles

17.3.1. Mesoporous silica nanoparticles

Mesoporous silica nanoparticles (MSN) have been widely studied in recent years due to their unique structure and ease with which the surface can be functionalized, allowing to develop a multifunctional platform that can be used for drug delivery (98-100) and as a novel gene transfection system (101-104). The development of advanced hybrid materials based on MSN has been mostly focused in the field of cancer therapy (104-110), often coupled to nucleic acid delivery (siRNA) to overcome cancer cells resistance to one or more chemotherapeutic agents (103). Fewer reports focused on the employ of MSN as drug delivery systems (DDS) for topical/dermatological applications (111-114).

The success of this material is testified by the impressive literature proliferation on the subject, which cannot be comprehensively reviewed in this contribution. Among the many relevant publications, interested readers can delve into the concept of ‘pharmaceutically adapted MSN platform’ by Meng et al. (109). Similarly, the drawing by Prof. Lindén and coauthors reproduced in Figure 17.4 summarizes the numerous cargo loading possibilities of MSNs (98, 110). MSNs have indeed all the peculiar properties of silica-based mesoporous materials (high surface area, ordered and tunable porosity, huge pore volume to accommodate and deliver large amounts of molecules, biocompatibility, etc.) (115), coupled to nanosize, which can be tuned in the range 50-200 nm.

These features allow to develop multifunctional nanocarriers, which can be targeted to cancer cells by both passive and active transport (specific cell targeting) in physiological fluids. Surface functionalization is employed to tune the surface charge, which influences the interaction with cell membranes and can decrease aggregation in water and biological media. MSN can thus carry drugs, nucleic acids, proteins, etc. coupled to magnetic materials to enable the particles to be used for T2 magnetic resonance imaging (MRI) and/or molecules for optical imaging (98, 99, 109).

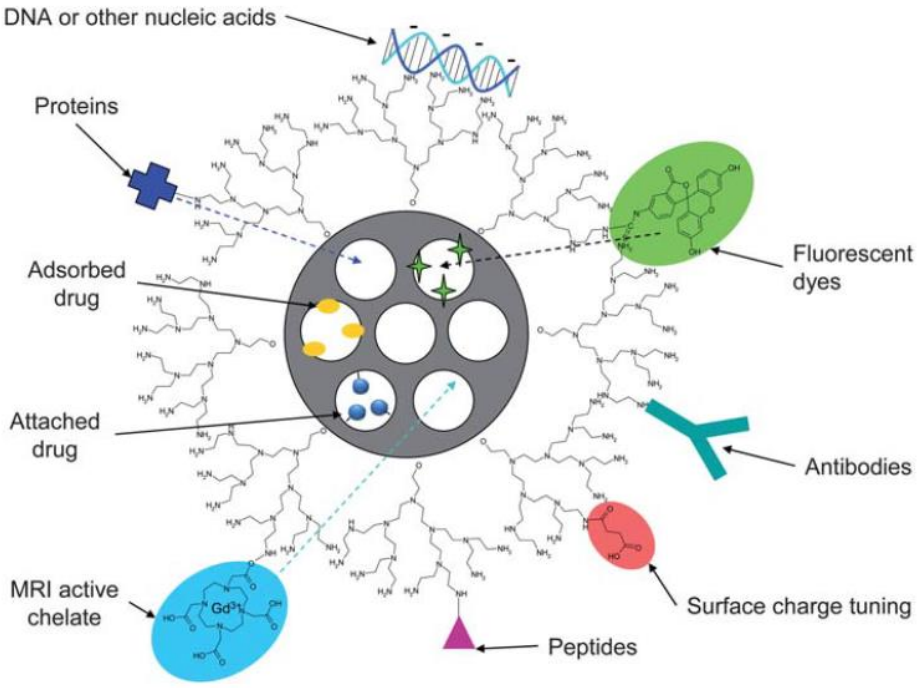

Figure 17 - 4 Pictorial representation of the many cargo loading possibilities of MSNs (Reproduced from Ref (98) with permission of The Royal Society of Chemistry).

From what mentioned above, it is clear that most reports about MSNs are not simply focused on their application for bioimaging, since agents for magnetic or optical imaging are often coupled to bioactive molecules, resulting in theranostic (therapy + diagnostics) systems (99, 116). Moreover, highly fluorescent molecules are often chosen as a cargo, since release from the pores can be tracked by fluorescence spectroscopy and microscopy (99, 109, 117-120). These includes either fluorescent dyes (that is without any therapeutic effect, only employed to check the material performance in terms of loading, release and cell internalization) or fluorescent drugs. Concerning the latter, doxorubicin (an anthracycline antibiotic) is a well-known anti-cancer (‘antineoplastic’ or ‘cytotoxic’) chemotherapy drug, widely employed as case study for DDS proof-of-concept (100, 104, 109, 121-124). For instance, doxorubicin was loaded into the pores of folate-functionalized MSNs, encapsulating highly sensitive ^{19}F MRI contrast agents, for active targeting of theranostic

systems (125). In another work, doxorubicin was employed on intrinsically fluorescent MSNs, doped with photosensitizing molecules, chlorin e6. This was aimed at designing imaging-guided combination therapy of cancer, including photodynamic and chemotherapy, achieving synergistic anti-tumor effects both *in vitro* and *in vivo* (126).

As fluorescent not-bioactive cargos are concerned, rhodamine B has been often employed, being one of the most readily available dye with a high absorption coefficient and quantum yield (117, 119, 127-129). For instance, rhodamine B was employed as cargo to test the potentiality of a redox-responsive release system based on hybrid copolymer/MSNs, with cleavable sulfide bonds. Moreover, the material was designed as a sensitive pH probe for cell/tissue imaging and clinical diagnosis, by further grafting of a fluorescent pH sensing monomer (1,8-naphthalimide) (129). In a different work, sulforhodamine B, hydrophobically modified sulforhodamine B, and Cascade Blue hydrazide were employed to obtain stable fluorescent MSNs, binding specific antibodies for diagnostic applications (130). Finally, rhodamine B as a fluorescent contrast agent was coupled in MSNs to verteporfin as a photosensitizer for PDT application. Specific attention was devoted to increase the fluorescence quantum yield and singlet oxygen delivery efficiency by controlling the dye dispersion and location within MSNs (131).

On the other hand, the release of rhodamine 6G from bare and amine-coated MSN has been studied at different pH values. This allowed the authors to demonstrate the effect of the electrostatic interactions between entrapped molecules and MSN charged surface on release kinetics (118). A similar pH dependent study was based on anionic molecules, namely fluorescent Orange II and sulfasalazine (an anti-inflammatory prodrug used for bowel disease), to study the application of MSNs as an oral delivery drug systems targeting at intestine (120).

One of the most commonly employed substances to fluorescently label MSNs for *in vitro* biocompatibility and trafficking studies is fluorescein isothiocyanate (FITC), which is a fluorescein molecule functionalized with an isothiocyanate group (-N=C=S). This derivative is reactive towards primary amine groups, and can be thus exploited to covalently link FITC to any kind of hybrid material bearing an amino group (122, 132-134). In an interesting work by Chen et al. a fluorescence ratiometric pH-sensor was developed loading on MSNs a pH sentitive dye (FITC) and rhodamine B isothiocyanate (RITC) as a reference one. This allowed to map the location of the MSNs through the site pH in HeLa cells, showing a charge mediated membrane-nanoparticle interaction mechanism (135). On the other hand, fluorescein was covalently linked to lipid bilayer

MSNs (LB-MSNs) with a double aim. First, biocompatibility and cell internalization of the nanocarriers could be investigated by fluorescence confocal spectroscopy and flow cytometry. Secondly, the controlled release of the fluorescent cargo was followed under disulfide reducing conditions (136). Similarly, fluorescein-based compounds were used as a cargo to investigate their stimulus-induced release from MSNs capped with poly(propylene imine) dendrimers, covalently linked to MSNs through cleavable disulfide bonds (137). In a very interesting report by Qian et al., fluorescein (hosted within MSN pores together with a black hole fluorescence quencher) was employed to test a MSN-based system for "off-on" switchable imaging. Intracellular activity could be checked by the design of wrapping DNA as a 'biogate' for a telomerase-responsive bioimaging system (138).

Another commercially available dye, Texas Red was employed to visualize cell internalization of polyamidoamine dendrimer-capped MSNs employed as novel for gene transfection systems (101). The same dye was covalently linked to MSNs, trapping cadmium sulfide (CdS) nanoparticles within their pores. The release of the photoluminescent quantum dots was followed by examining the fluorescence resonance energy transfer between the two species (139). In this context it is also worth to mention the report about enhanced green fluorescent protein (eGFP), coupled to fluorescently labeled bovine serum albumin (BSA), loaded in gold nanoparticle functionalized MSNs. These were employed as a proof-of-concept to test the co-delivery of active, non-denatured proteins and plasmid DNA to plant tissues (140).

From what is described above, it is clear that the development of MSNs in the field of optical imaging is often coupled to other aspects, such as the design of stimuli-responsive, 'off-on' systems, coupling advanced diagnostics to innovative therapeutic approaches. This means that in most of the works mentioned above the properties of the fluorescent dyes, their optimization in terms of structure, emission intensity/wavelength, and their incorporation into the silica based material were often in the background. Some of these aspects were explored in other works, including the exploration of new and improved fluorescent agents in hybrid MSN-based nanomaterials, or their optimization for specific applications. Some of the more interesting works will be shortly reviewed in the following.

Concerning specific applications, poly-(lactic acid)-coated MSNs (PLA-MSN) were proposed as a fluorescent probe for the selective detection of extracellular amino acid-based neurotransmitters (e.g. dopamine, tyrosine and glutamic acid). PLA was employed as a gatekeeper, to control the

neurotransmitter molecules diffusion in and out of the pores. Fluorescence-sensing properties were obtained by grafting of o-phthalic hemithioacetal groups (OPTA), reacting with the primary amines of the neurotransmitters to form fluorescent isoindole products (Fig. 17.5) (141). In another work, a fluorescent nanosensor for real-time imaging of the fluctuations of mitochondrial hydrogen peroxide (H_2O_2) and pH in living cells was developed, since these parameters are closely related with important mitochondrial dysfunctions. The MSN-based material design included functionalization with triphenylphosphonium for mitochondria targeting, and loading of two fluorescent probes, namely Cy-O-she - a specifically synthesized NIR fluorescent probe - and fluorescein. Loading of the two molecules in a single targeting nanocarries allowed for simultaneous monitoring of H_2O_2 and pH changes using a single fluorescent probe (142).

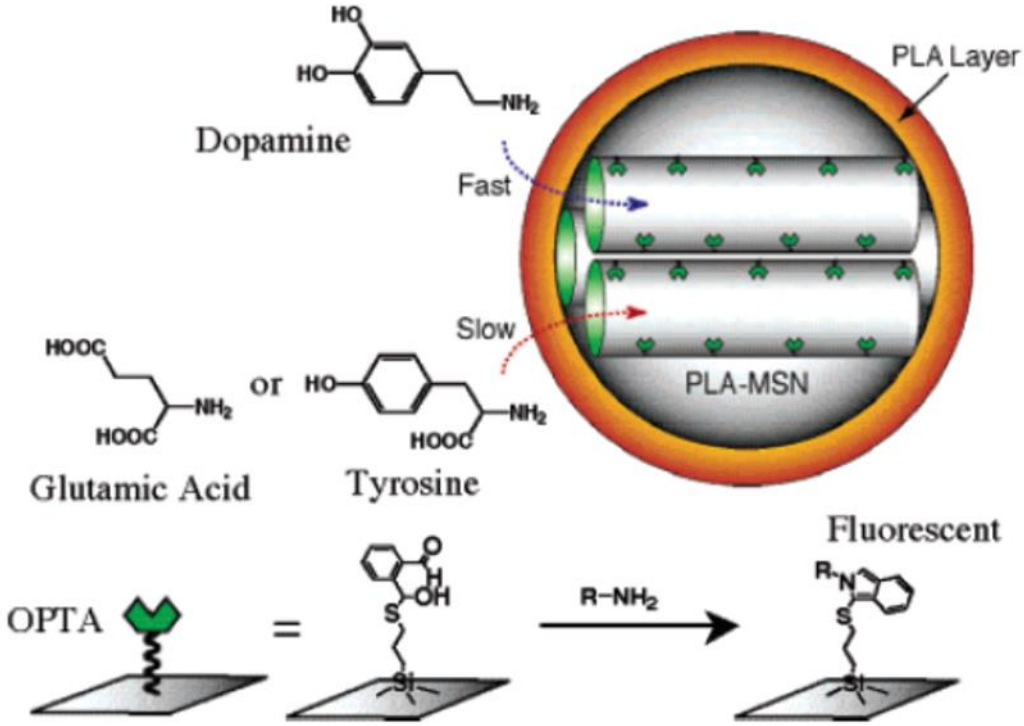

Figure 17 - 5 Schematic representation of PLA-coated MSNs functioning as selective fluorescent sensor for amino-based neurotransmitters. (Adapted with permission from ref. (141). Copyright 2004 American Chemical Society).

The high accessible volume and versatility of MSN-based nanocarriers to host different functionalities was exploited by Zhang et al. for dual-modality imaging (*in vivo* fluorescence and MRI). Ru/Gd-Al@MSNs systems were prepared by loading through simple ion-exchange the fluorescent tris(bipyridine)ruthenium(II) cation into Gd^{3+} and Al^{3+} doped MSN. The material was tested with a mouse model, showing good biocompatibility, intense red fluorescence and enhanced MR imaging efficiency with respect to commercial contrast agents (143). A very promising approach was proposed by Zeng et al. for intraoperative fluorescence molecular imaging, specifically applied to liver cancer surgical intervention. An arginine-glycine-aspartic acid (RCG)

conjugated MSN was loaded with NIR emitting indocyanine green dye. This new probe allowed to detect microtumors and satellite lesions measuring less than 1 mm in living mice, with an excellent tumor-to-normal tissue contrast. This excellent result was ascribed to the high loading of dye into the MSN nanocarrier coupled to the RCG-mediated tumor specificity (144). An improved NIR emitting fluorescent dye, ATTO647N, was found to be twice as bright as Cy5.5 in aqueous solutions and stable enough to be employed in the co-condensation synthesis of MSNs. This was the basis to develop a multifunctional theranostic system coupling fluorescence imaging, therapy (loading a palladium-porphyrin based photosensitizer for photodynamic therapy) and targeting, employing cRGDyK peptides for cancer cells internalization (107).

Concerning less conventional fluorescent agents, we report about the incorporation of a fluorescent conjugated polymer, poly(p-phenylenevinylene) (PPV) in MSNs. Core shell systems were obtained by growing a further shell of MSNs on the fluorescent hybrid PPV-MSNs. The material showed good performance in drug loading/release, high luminescence stability and nontoxicity in bioimaging studies on Hela cells (145). Another example is represented by aggregation induced emission (AIE) materials, which, contrarily to conventional organic dyes, emit more efficiently while in aggregated state than in dispersed one. A MSNs-based nanocarrier incorporating an example of AIE (An18, a derivative of 9,10-distyrylanthracene) showed uniform morphology, a strong green-yellow fluorescence and an excellent biocompatibility with A549 cells (146). Other interesting works report on the use of grafted fluorescent graphene quantum dots (GQDs) (147), or photoluminescent nanodiamond (ND) cores in MSN-based core-shell systems (148, 149). Even if this review is not exhaustive, it is sufficient to demonstrate the huge research efforts in the field, coupled to the great versatility and potential of the MSN-based nanoplatforms.

17.3.2. Fluorescent Organosilicas

Mesoporous organosilicas doped with fluorescent moieties are attracting hybrid materials for bioimaging applications due to the combination of the unique textural features of mesoporous ordered silica (high surface area and uniform pore sizes) with the tunable surface polarity due to the presence of the organic groups, that can be luminescent, incorporated in the silica framework. In particular, periodic mesoporous organosilicas (PMOs) synthesized at the end of last century (150, 151), represent a new class of functional or multifunctional materials having an organic-inorganic hybrid framework and ordered mesopores. The incorporation of luminescent organic molecules in such a type of materials guarantees a high dispersion of the organic functionalities avoiding the

presence of non-emissive aggregates (152). PMOs are synthesized from 100% or less organic-bridged alkoxysilane precursors [$(R'O)_3Si\text{-}R\text{-}Si(OR')_3$] allowing the introduction of a huge variety of organic functionalities by changing the R group (153). For application in nanomedicine, it is necessary to synthesize PMOs in the nanometric range (154). Great scientific efforts have been done recently in the synthesis of nanosized PMOs, in fact the nanoparticle size governs their biological interactions and lifespan with parameters such as good suspension in solution, cellular uptake, blood circulation, tumor accumulation (Fig. 17-6) (155).

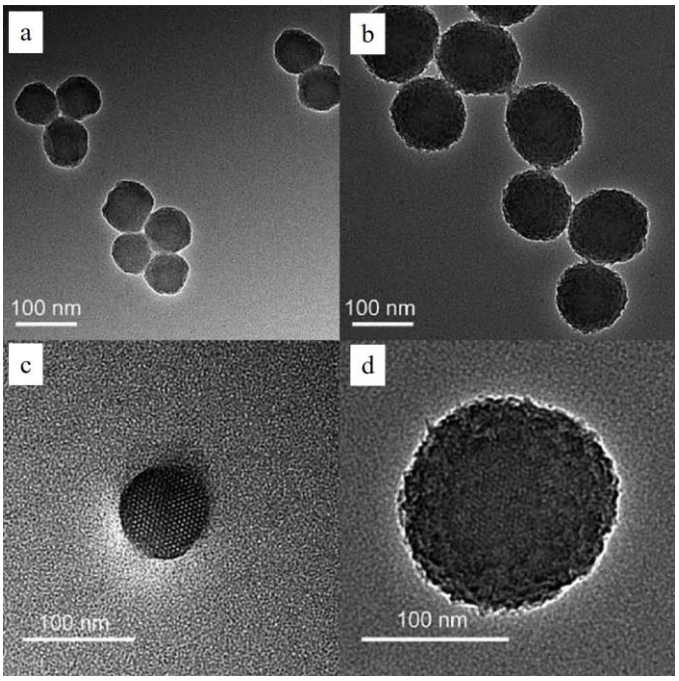

Figure 17 - 6 TEM images of (a) ethenylene–PMO nanoparticle at low magnification, (b) phenylene–PMO nanoparticle at low magnification, (c) ethenylene–PMO nanoparticle along the channel direction and (d) phenylene–PMO nanoparticle at high magnification. (Adapted from Ref. (155) with permission of the Royal Society of Chemistry).

Nanometer-sized fluorescent PMOs represent nowadays a viable alternative to the use of MSNs, in fact the fluorophores can be located simultaneously in the silica framework and in the mesochannels promoting excitation energy transfer from the framework donors to the acceptors in the channels. In addition, the possibility to densely pack the fluorescent moieties in the PMO framework enhances both light absorption and luminescence intensities (156). Tani *et al.* reviewed the synthetic pathways of luminescent PMOs following two approaches: co-condensation of fluorophores having alkoxysilyl groups and a large quantity of silica precursors such as tetraethylorthosilicate (Fig.17-7a) and 100% fluorophore-bridged organosilane precursors (Fig.17-7b) (152).

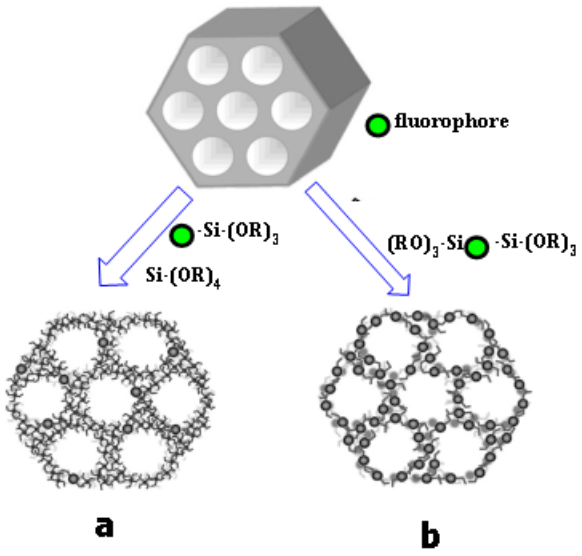

Figure 17 - 7 Different synthetic strategies to prepare fluorescent PMOs: a) co-condensation of fluorophores having alkoxysilyl groups; b) 100% fluorophore-bridged organosilane precursor (Adapted from Ref. (152) with permission of the Royal Society of Chemistry).

Between the two synthesis procedures, the co-condensation is the most followed due to the production of highly ordered mesostructures and a high dispersion of the fluorophore molecules into the PMO network avoiding self-quenching. One of the first reports of the use of 100% fluorophore precursors approach is the synthesis of luminescent-PMO using bis(propyl iminomethyl)phenol-bridged organosilane reported by Chandra et al. (157). Other examples of a different luminescence behavior when the fluorophore molecules are inserted into the PMO framework is represented by the fluorescence properties of benzene, biphenyl, naphthalene and anthracene in PMOs investigated by Goto *et al.* (156). In particular, the fluorescence spectra of the solids were red-shifted as compared to those of the precursors and the fluorescence quantum yields were lower with the exception of biphenyl-PMO. This fluorescence enhancement has been attributed to a restriction of the intramolecular rotational vibration of the biphenyl groups present in the dense packing structure. In addition the absorption coefficient was found to be considerably higher than for dye doped mesoporous silica. Despite the great scientific efforts in the optimization of the synthetic procedures to produce highly luminescent organosilicas, only recently these new luminescent systems were applied in the field of nanomedicine for optical imaging and drug delivery; nevertheless in contrast to the conventional silica-based materials, the cytotoxicity and bio-safety of PMOs nanoparticles are not yet deeply investigated through extensive and detailed *in vitro* and *in vivo* research (158).

The peculiar physical-chemical properties of PMOs nanoparticles allow hosting simultaneously more than one fluorophore. Three types of fluorophores at various ratios and with a good dispersion have been embedded within the PMO framework by D. Lu *et al*. to obtain a multicolor emission nanosystem by a single wavelength excitation (159). Bis-silylated biphenyl (Biph), anthracene (Anth) and naphthalimide (Naph) were used as energy donor, intermediate and terminal acceptor to build fluorescence resonance energy transfer (FRET) cascades. These dyes were chosen due to a good overlap between the emission spectra of energy donor and the excitation spectra of the acceptor. The tunable fluorescence property of the triple-dye doped PMO nanoparticles was studied by varying the dye ratio between FRET tandems. When the ratio of the three dyes was 1:1:1, the emission spectrum of the system showed three peaks centered at 320 (Biph), 460 (Anth) and 520 (Naph) nm by using the absorption wavelength of Biph at 280 nm (Fig. 17-8). The FRET occurs due to the short distance between energy donor and acceptor in the nanometer-size thick framework wall (Fig.17.8D). The particular arrangement of the dyes inside the framework wall preserves the pore accessibility allowing the use of such nanoplatforms not only as bio-imaging agents but also as drug carriers. The multi-fluorescent PMO nanoparticles were also tested *in vitro* using living HeLa cells as colorful bioimaging agents that benefit from the FRET mechanism. The cell viability was also monitored indicating a good biocompatibility of PMO nanoparticles.

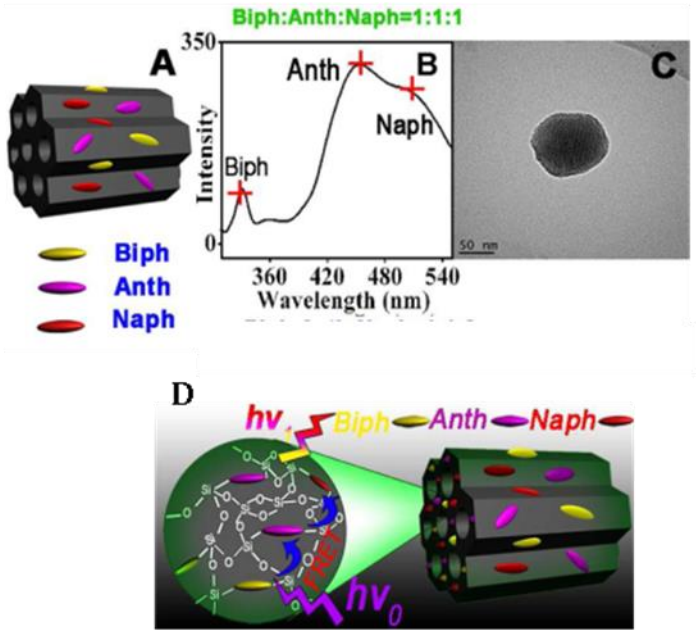

Figure 17 - 8 Representation (A), emission spectrum (B), TEM image (C) and FRET by a single wavelength excitation (D) of triple-dye PMO nanoparticles with 1:1:1 ratio. (Adapted with permission from ref. (159). Copyright 2012 American Chemical Society).

Another paper highlighting the potential role of mesostructured organosilicas in bioimaging applications reports the coupling of ACQ (aggregation-caused quenching) dye with fluorophores that have aggregation-induced emission (AIE) (160). The ACQ dyes are conventional fluorophores such as fluorescein, rhodamine and cyanine derivatives that suffer from concentration quenching due to the aggregation when they are present in concentrated solutions or in the solid state. For this reason, a careful control of the dye loading, avoiding aggregation, is necessary to obtain a system with high quantum yield and high emission efficiency. In contrast, AIE dyes represent a novel class of fluorophores with an enhanced emission in the solid state due to the effective restriction of intramolecular rotations (89). Generally, due to their opposite luminescent behaviors, AIE and ACQ systems are not easily coupled to build an efficient fluorescent material. The PMO nanoparticles offer the possibility to host concomitantly AIE and ACQ fluorophores located in different positions; the coupling of AIE and ACQ dyes is important to produce new donor-acceptor systems based on FRET with multicolor emission (Fig. 17-.9). Blue-emitting TPE-bridged organosilane (AIE fluorophore) was used as precursor to synthesize PMO nanoparticles; the AIE-PMOs represent the energy donors. As energy acceptor, ACQ dyes as rhodamine B (RhB) and rhodamine 6G (R6G) were used and were encapsulated in the mesopores of AIE-PMO.

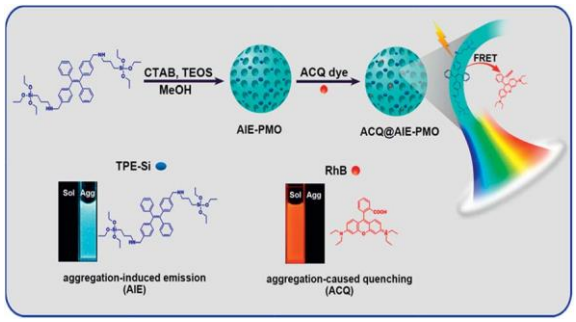

Figure 17 - 9 Schematic illustration of the synthesis of ACQ@AIE-PMO with tuneable multicolour emission. AIE-PMO nanospheres are prepared by using AIE-active TPE-Si as a precursor, where TPE units are covalently embedded within the framework forming the pore walls; ACQ molecules (RhB) are then encapsulated in the mesoporous channels of the AIE-PMO. Note that the TPE-Si precursor is nonemissive in solution but luminesces intensively upon molecular aggregation, while RhB dye is emissive in solution but suffers from aggregation-caused fluorescence quenching. (Reproduced from Ref. (160) with permission of the Royal Society of Chemistry).

The resulting ACQ@AIE-PMOs shows multicolor emission over a wide range of the visible spectrum with high quantum yields. The red-emitting RhB has a good spectral overlap with the emission band of the AIE-PMOs. The energy transfer from the AIE-PMO framework and the encapsulated RhB was demonstrated by fluorescence spectroscopy coupled with emission lifetimes

that are strictly dependent on the RhB loading. The emission color of the composite PMO changes from blue to red *via* white light under UV irradiation. Moreover, the quantum yield of the RhB@AIE-PMO system showed an enhancement due to the direct energy transfer from the AIE unit to the ACQ dye present in the mesochannels without a radiation-reabsorption process. These new systems were also evaluated with HeLa cells for *in vitro* cellular imaging. These studies evidenced that the luminescent nanoparticles were successfully internalized into the cells and strong blue, white and red light emissions were observed under the confocal microscope.

The PMO nanoparticles merge efficiently the advantages of inorganic silica, of the mesopores and organic molecules and represent a potential nanoplatform to produce advanced theranostic delivery nanosystems for biomedical applications.

17.4. Zeolites

Zeolites are crystalline microporous alluminosilicates which are extremely exploited as catalysts for oil refining, petrolchemistry and organic synthesis of fine and specialty chemicals, particularly pharmaceuticals intermediates (161). The key properties which make these materials particularly appealing for catalysis applications are *(i)* high surface area and adsorption capacity *(ii)* the possibility of tuning the adsorption properties by changing the hydrophilicity/hydrophobicity balance of the framework and *(iii)* the possibility of tailoring strength and concentration of active sites. Furthermore, the size of their channels and cavities well fits with many small molecules of interest and the intricate channel structure provides to zeolite an excellent shape selectivity (162). All these features, which are of paramount importance in catalysis, are as well interesting for their application in the design and preparation of optical materials. The ability to host various organic and inorganic species while being transparent in the UV-Vis-NIR makes zeolites ideal host materials for supramolecular organization and in many cases the confinement of molecules in zeolites leads to interesting photophysical and photochemical phenomena which are not observable in solution (163). As a consequence, in recent years they have attracted attention for the preparation of novel materials designed at the nanoscale level, in particular in the area of the development of optical materials where pre-defined distances or a specific spatial pattern of the guests is required in order to obtain a particular optical response (164). Most of the examples reported in the literature concern the supramolecular organization of dyes within the channels of zeolites with the aim of producing highly efficient antenna materials to be used as luminescence solar concentrators (165). Although the design, preparation and characterization of this kind of materials is very interesting

and can offer useful hints for the optimization of fluorescence performances of hybrid materials, these applications cannot be reviewed in this contribution as they are referred to micrometer-sized zeolite crystals which rarely fit with bioimaging applications. The interested reader can refer to extensive literature on the topic (166-168). 1D nanochannel systems are more studied than 2D and 3D systems as it is relatively easier to control fluorophores loading and diffusion in simpler systems. Among the most exploited 1D nanochannel hosts for the preparation of host-guest composites, ALPO-5, zeolite L (ZL), MFI silicalite-1 and ZSM-5 have been the most successful (167); MFIs are actually not 1D channels host but have often been handled as such because of the different diameters of the two arrays of perpendicularly oriented channels. The largest variety of 1D-guest zeolite composites with interesting and controllable optical properties has been prepared by using ZL as host, mainly because of the possibility of adjusting size of the particles in the range 30 nm-10 μm and the morphology from elongated barrel-shaped crystals to discs (167, 169, 170). The general structure of ZL crystal is reported in Fig. 17-10. The primary building unit of the hexagonal ZL framework consists of TO_4 tetrahedrons (T= Al or Si) which form 1D channels running parallel to the crystal c axis. The negative charge caused by the Al atoms is compensated by monovalent cations (M^+, usually K^+ or Na^+). It is useful to imagine a single ZL crystal as a bunch of parallel channels having apertures of 0.71 nm and the largest diameter inside the channel being 1.26 nm. Composites synthesized by embedding molecules, complexes, and clusters into the one-dimensional channels of ZL (165) have been reported, showing a large variety of different properties which make these systems promising objects for use in analytics, biology, diagnostics and drug delivery.

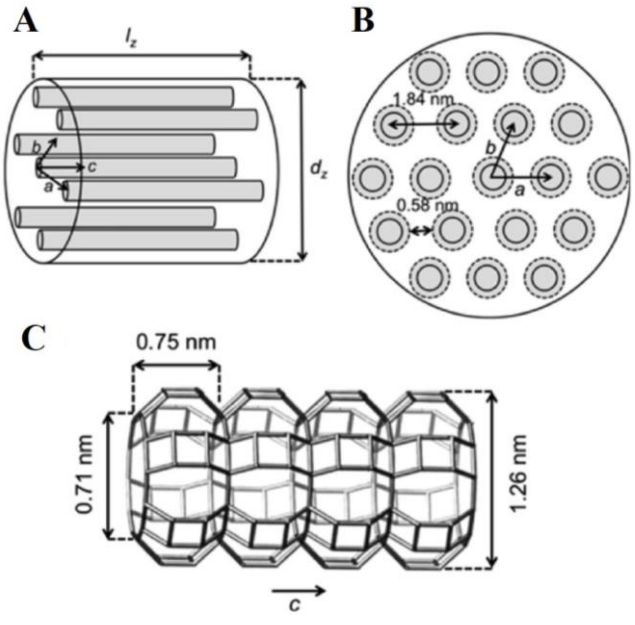

Figure 17 - 10 Representation of a single crystal as a cylinder with a system of 1D parallel channels (depicted as gray tubes). B. Schematic representation of the basal surface of ZL crystals (solid lines represent pore openings; dashed lines show the largest channel diameter). C. Side view of one ZL channel. (Adapted with permission from Ref. (165). Copyright 2013 American Chemical Society).

De Cola and coworkers (171) prepared disc-shaped ZL crystals smaller than 200 nm, loaded with a green-emitting fluorophore, namely N,N'-bis(2,6-dimethylphenyl)perylene-3,4,9,10-tetracarboxylic diimide (DXP), and functionalized on the external surface with Anti-DIG (digoxygenin) antibodies, to be employed in microarray fluorescence immunoassays. DXP was selected because of its molecular size, which is comparable with the channel size, thus limiting the possibility of aggregation inside the channels. Furthermore, DXP is strongly hydrophobic, so it can be inserted in the ZL channels by gas-phase insertion methods and no leakage is expected in buffer solutions during conjugation, storage and assays performing. The authors proved that ZL nanoparticles with encapsulated DXP molecules have bright fluorescence properties which can be used for immunoassay quantifications. Furthermore, the external surface of the nanocrystals is available for further modification and immobilization of antibodies, which retained their binding ability ensuring high-sensitivity performances.

Ion-exchange procedure, instead of gas-phase insertion, was used for the loading of water soluble dye pyronine within the channels of barrel-shaped ZL crystals (172). The loaded dye maintained the absorption and emission features, without occurring of quenching or aggregation phenomena. The authors were then able to functionalize the channel entrance (173) with thousand molecules of amino-derivatives, which are protonated under physiological conditions, leading therefore to positively charged systems. Amino-functionalized fluorescent ZL crystals were then incubated with *E. coli* bacteria in phosphate buffer, leading to the stable formation of ZL-bacteria assembly, most probably owing to electrostatic interactions. As expected, non-functionalized ZL crystals do not form stable assemblies with bacteria. Formation and evolution of assemblies was easily followed by fluorescence microscopy thanks to the green emission of the pyronine guest. The authors demonstrated that the self-assembly of living systems and functional materials is possible by a detailed design of the materials and further engineering of the nanosystems can lead to couple self-assembly with the exchange of specific information between the zeolite and the bacteria (small molecules, ions, etc.). Another interesting example of self-assembly of ZL on living systems, even if obtained with micrometer-sized zeolites, is reported by Bossart (174) who observed that when the petals of different flowers were immersed into a suspension containing dye-loaded ZL crystals, the latter align into patterns which are distinct for each flower species. The possibility of monitoring alignment pattern arises from the peculiar arrangement of fluorophores within the channels of ZL

crystals. Methincyanine (Mc^+) and oxonine (Ox^+) were loaded into the ZL; the blue fluorescent Mc^+ is aligned parallel to the zeolite channels, whilst Ox^+, being smaller in size, is aligned almost perpendicular with respect to the channels (175). In both cases polarized microscopy analyses allowed to investigate the alignment pattern of the ZL crystals, which is really interesting as the visualization of surface patterns by means of optical microscopy methods, which are less destructive than other tools such as electron microscopy, may also be applied to living organisms. The phenomenon may also contribute to the application of drugs at specific places, and we can learn from these observations how to pattern a surface in order to realize self-organization of micro- or nano-objects. Barrel-shaped 30 nm-long ZL crystals have been engineered in order to act as two-component FRET systems (176). Pyronine (Py) and Texas Red (TR) were chosen as the donor and acceptor, respectively, because of the favorable spectral overlap between the fluorescence spectrum of Py and the absorption spectrum of TR. Furthermore, the fluorescence maximum of TR (612 nm) is well separated from that of Py (510 nm), ensuring no interference and good spectra resolution. Py was loaded into the ZL channels by ionic exchange to a loading level of about 10%, which was optimized on the basis of previous experiment. Due to its bulky structure which cannot enter the channels, TR, if properly modified, can be used as a stopcock molecule, both acting as FRET acceptor and preventing Py leakage. Stopcock molecules, in fact, consist of a head, a spacer and a label; only the spacer and the label can enter the channels, while the head part is too bulky to enter the pore opening. Depending on the reactivity of the label. The stopcock molecule can be attached either reversibly or irreversibly. In order to use TR molecule both as a FRET acceptor and as a stopcock molecule, the authors modified the channel entrance of Py-loaded ZL by grafting with aminopropyltriethoxysilane followed by a reaction with methyl-3-isothiocyanopropionate, leading exposed carboxyester groups. TR, in the form of Texas red hydrazide, was then coupled to the carboxyester functionalized zeolite. In such architecture, as shown in Fig. 17.11, excitation energy is funneled from Py dyes inside the ZL channels to TR acceptor located at the outside. Due to the very large number of fluorescent molecules which can be loaded into ZL channels and used as FRET pairs, this approach can be considered very versatile and can lead to highly tunable organized materials, offering the opportunity of exploring energy transfer phenomena and developing new fluorescent probes.

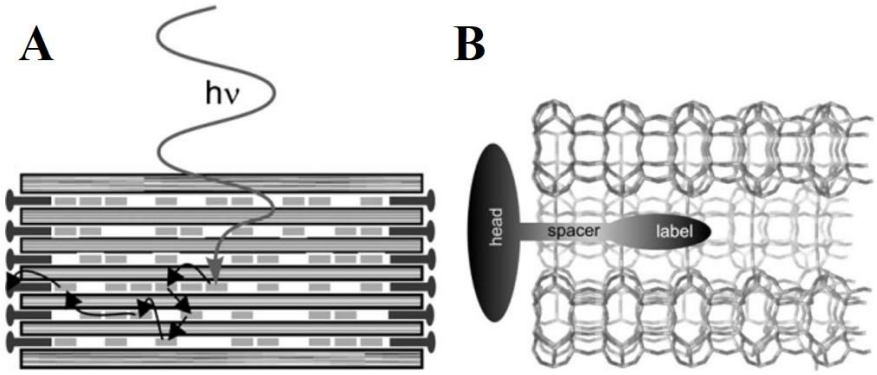

Figure 17 - 11 A. Representation of a ZL crystal loaded with Py donor molecules and modified with TR acceptor stopcocks at the channel openings. B. Enlargement showing details of the channel and of a stopcock molecule. Only the spacer and the label are small enough to enter the channel. (Reproduced with permission from Ref.(176). Copyright 2006 Elsevier Inc.).

References

1. Sanchez C, Ribot F. Design of hybrid organic-inorganic materials synthesized via sol-gel chemistry. New J Chem. 1994;18:1007-47.
2. Chauhan BPS, Editor. Hybrid Nanomaterials: Synthesis, Characterization, and Applications: John Wiley & Sons, Inc.; 2011. 334 p.
3. Rurack K, Martinez-Manez R, Editors. The Supramolecular Chemistry of Organic-Inorganic Hybrid Materials: John Wiley & Sons, inc.; 2010. 766 p.
4. Tea BK, Editor. Functional Hybrid Nanomaterials: Design, Synthesis, Structure, Properties, And Applications. [In: Coord. Chem. Rev., 2009; 253(23-24)]: Elsevier B.V.; 2009. 281 p.
5. Kickelbick G, Editor. Hybrid Materials: Synthesis, Characterization, and Applications: Wiley-VCH Verlag GmbH & Co. KGaA; 2007. 498 p.
6. Antonietti M, Chaudret B, Drillon M, Etourneau J, Sanchez C, Subramanian M, et al. Special Issue: Advanced Functional Nanomaterials - from Nanoscale Objects to Nanostructured Inorganic and Hybrid Materials. (Proceedings of the 2005 European Materials Research Society Meeting held 31 May-3 June 2005 in Strasbourg, France.) [In: Prog. Solid State Chem.; 2006, 33(2-4)]: Elsevier Ltd.; 2006. 275 p.
7. Comez-Romero P, Sanchez C, Editors. Functional Hybrid Materials: Wiley-VCH Verlag GmbH & Co. KGaA; 2004. 417 pp. p.
8. Patel V, Papineni RVL, Gupta S, Stoyanova R, Ahmed MM. A realistic utilization of nanotechnology in molecular imaging and targeted radiotherapy of solid tumors. Radiat Res. 2012;177:483-95.
9. Lucas M, Riedo E. Combining scanning probe microscopy with optical spectroscopy for applications in biology and materials science. Rev Sci Instrum. 2012;83(Copyright (C) 2012 American Chemical Society (ACS). All Rights Reserved.):061101/1-/35.
10. Peti-Peterdi J, Burford JL, Hackl MJ. The first decade of using multiphoton microscopy for high-power kidney imaging. Am J Physiol. 2012;302( ):F227-F33.
11. Johnston LJ. Fluorescence imaging on the nanoscale: bioimaging using near-field scanning optical microscopy. Photochemistry. 2011;39(Copyright (C) 2012 American Chemical Society (ACS). All Rights Reserved.):191-210.
12. Ntziachristos V. Going deeper than microscopy: the optical imaging frontier in biology. Nat Methods. 2010;7(Copyright (C) 2012 American Chemical Society (ACS). All Rights Reserved.):603-14.
13. Huff TB, Shi Y, Fu Y, Wang H, Cheng J-X. Multimodal nonlinear optical microscopy and applications to central nervous system imaging. IEEE J Sel Top Quantum Electron. 2008;14(Copyright (C) 2012 American Chemical Society (ACS). All Rights Reserved.):4-9.
14. Wabuyele MB, Vo-Dinh T, editors. Nanoimaging of biomolecules using near-field scanning optical microscopy. 2007: CRC Press LLC.
15. Kawata S, Inouye Y, Ichimura T. Near-field optics and spectroscopy for molecular nano-imaging. Sci Prog (St Albans, U K). 2004;87(Copyright (C) 2012 American Chemical Society (ACS). All Rights Reserved.):25-49.
16. Bragas AV, Scarpettini AF, Masip M, editors. Optical nanoimaging with plasmonic probes. 2010: American Chemical Society.
17. Sokolov K, Follen M, Aaron J, Pavlova I, Malpica A, Lotan R, et al. Real-time vital optical imaging of precancer using anti-epidermal growth factor receptor antibodies conjugated to gold nanoparticles. Cancer Res. 2003;63(Copyright (C) 2012 American Chemical Society (ACS). All Rights Reserved.):1999-2004.
18. Elliott AM, Stafford RJ, Schwartz J, Wang J, Shetty AM, Bourgoyne C, et al. Laser-induced thermal response and characterization of nanoparticles for cancer treatment using magnetic

resonance thermal imaging. Med Phys. 2007;34(Copyright (C) 2012 American Chemical Society (ACS). All Rights Reserved.):3102-8.
19. Gao J, Gu H, Xu B. Multifunctional Magnetic Nanoparticles: Design, Synthesis, and Biomedical Applications. Accounts of Chemical Research. 2009;42(8):1097-107.
20. Xu W, Kattel K, Park JY, Chang Y, Kim TJ, Lee GH. Paramagnetic nanoparticle T1 and T2 MRI contrast agents. Phys Chem Chem Phys. 2012;14:12687-700.
21. Wallnofer EA, Thurner GC, Abdelmoez AA, Rohr I, Klammsteiner N, Talasz H, et al. MRI molecular imaging with nanoparticles: a technical platform for early diagnosis of cancer. Int J Clin Pharmacol Ther. 2011;49(Copyright (C) 2012 U.S. National Library of Medicine.):73-4.
22. Kircher MF, Willmann JK. Molecular body imaging: MR imaging, CT, and US. part I. principles. Radiology. 2012;263:633-43.
23. Wang C-H, Huang Y-F, Yeh C-K. Aptamer-Conjugated Nanobubbles for Targeted Ultrasound Molecular Imaging. Langmuir. 2011;27(Copyright (C) 2012 American Chemical Society (ACS). All Rights Reserved.):6971-6.
24. Ke H, Wang J, Dai Z, Jin Y, Qu E, Xing Z, et al. Gold-Nanoshelled Microcapsules: A Theranostic Agent for Ultrasound Contrast Imaging and Photothermal Therapy. Angew Chem, Int Ed. 2011;50(Copyright (C) 2012 American Chemical Society (ACS). All Rights Reserved.):3017-21, S/1-S/5.
25. Deshpande N, Willmann JK, editors. Microparticle- anmd nanoparticle-based contrast-enhanced ultrasound imaging contrast-enhanced ultrasound imaging. 2011: John Wiley & Sons, Inc.
26. Wang Y-H, Liao A-H, Chen J-H, Lee Y-H, Wang C-R, Li P-C. Thermotherapy with a photoacoustic/ultrasound dual-modality agent. Proc SPIE. 2011;7899(Copyright (C) 2012 American Chemical Society (ACS). All Rights Reserved.):78993V/1-V/5.
27. Caissie A, Karshafian R, Hynynen K, Czarnota GJ. Ultrasound contrast microbubbles: in vivo imaging and potential therapeutic applications. Pan Stanford Ser Biomed Nanotechnol. 2011;2(Copyright (C) 2012 American Chemical Society (ACS). All Rights Reserved.):267-91.
28. Devaraj NK, Keliher EJ, Thurber GM, Nahrendorf M, Weissleder R. 18F Labeled Nanoparticles for in Vivo PET-CT Imaging. Bioconjugate Chem. 2009;20(Copyright (C) 2012 American Chemical Society (ACS). All Rights Reserved.):397-401.
29. Werner MK, Schmidt H, Schwenzer NF. MR/PET: A New Challenge in Hybrid Imaging. American Journal of Roentgenology. 2012;199(2):272-7.
30. Lee H-Y, Li Z, Chen K, Hsu AR, Xu C, Xie J, et al. PET/MRI dual-modality tumor imaging using arginine-glycine-aspartic (RGD)-conjugated radiolabeled iron oxide nanoparticles. J Nucl Med. 2008;49(Copyright (C) 2012 American Chemical Society (ACS). All Rights Reserved.):1371-9.
31. Phelps ME. Positron emission tomography provides molecular imaging of biological processes. Proc Natl Acad Sci U S A. 2000;97(Copyright (C) 2012 American Chemical Society (ACS). All Rights Reserved.):9226-33.
32. Sensale-Rodriguez B, Yan R, Kelly MM, Fang T, Tahy K, Hwang WS, et al. Broadband graphene terahertz modulators enabled by intraband transitions. Nat Commun. 2012;3(Copyright (C) 2012 U.S. National Library of Medicine.):780.
33. Patil RR, Yu J, Banerjee SR, Ren Y, Leong D, Jiang X, et al. Probing In Vivo Trafficking of Polymer/DNA Micellar Nanoparticles Using SPECT/CT Imaging. Mol Ther. 2011;19(Copyright (C) 2012 American Chemical Society (ACS). All Rights Reserved.):1626-35.
34. Kryza D, Taleb J, Janier M, Marmuse L, Miladi I, Bonazza P, et al. Biodistribution Study of Nanometric Hybrid Gadolinium Oxide Particles as a Multimodal SPECT/MR/Optical Imaging and Theragnostic Agent. Bioconjugate Chemistry. 2011;22(6):1145-52.
35. Yelin D, Oron D, Thiberge S, Moses E, Silberberg Y. Multiphoton plasmon-resonance microscopy. Optics express. 2003;11(12):1385-91. Epub 2003/06/16.

36. Wang C, Kim J, Jin CT, Leong PHW, McEwan A. Near infrared spectroscopy in optical coherence tomography. J Near Infrared Spectrosc. 2012;20(Copyright (C) 2012 American Chemical Society (ACS). All Rights Reserved.):237-47.
37. Rodriguez-Lorenzo L, Fabris L, Alvarez-Puebla RA. Multiplex optical sensing with surface-enhanced Raman scattering: A critical review. Anal Chim Acta. 2012;745(Copyright (C) 2012 American Chemical Society (ACS). All Rights Reserved.):10-23.
38. Hankus ME, Cullum BM. SERS nano-imaging probes for characterizing extracellular surfaces. Proc SPIE-Int Soc Opt Eng. 2007;6759(Copyright (C) 2012 American Chemical Society (ACS). All Rights Reserved.):675908/1-/10.
39. Hankus ME, Cullum BM. SERS probes for the detection and imaging of biochemical species on the nanoscale. Proc SPIE-Int Soc Opt Eng. 2006;6380(Copyright (C) 2012 American Chemical Society (ACS). All Rights Reserved.):638004/1-/12.
40. Vo-Dinh T, Wang H-N, Scaffidi J. Plasmonic nanoprobes for SERS biosensing and bioimaging. J Biophotonics. 2010;3:89-102.
41. Kiser JB, Cullum BM, Porterfield DM, Booksh KS. Optical cross-talk and surface characterization of SERS nanoimaging bundle substrates. Proc SPIE. 2010;7674(Copyright (C) 2012 American Chemical Society (ACS). All Rights Reserved.):76740D/1-D/8.
42. Zaman RT, Diagaradjane P, Wang JC, Schwartz J, Rajaram N, Gill-Sharp KL, et al. In vivo detection of gold nanoshells in tumors using diffuse optical spectroscopy. IEEE J Sel Top Quantum Electron. 2007;13(Copyright (C) 2012 American Chemical Society (ACS). All Rights Reserved.):1715-20.
43. Majumdar D, Peng X-H, Shin DM. The medicinal chemistry of theragnostics, multimodality imaging and applications of nanotechnology in cancer. Curr Top Med Chem (Sharjah, United Arab Emirates). 2010;10(Copyright (C) 2012 American Chemical Society (ACS). All Rights Reserved.):1211-26.
44. Le Trequesser Q, Seznec H, Delville M-H. Functionalized nanomaterials: their use as contrast agents in bioimaging: mono- and multimodal approaches. Nanotechnol Rev. 2013;2:125-69.
45. Arap W, Pasqualini R, Montalti M, Petrizza L, Prodi L, Rampazzo E, et al. Luminescent Silica Nanoparticles for cancer diagnosis. Current medicinal chemistry. 2013;20(17):2195-211.
46. Quan B, Choi K, Kim Y-H, Kang KW, Chung DS. Near infrared dye indocyanine green doped silica nanoparticles for biological imaging. Talanta. 2012;99(0):387-93.
47. Huang X, Zhang F, Lee S, Swierczewska M, Kiesewetter DO, Lang L, et al. Long-term multimodal imaging of tumor draining sentinel lymph nodes using mesoporous silica-based nanoprobes. Biomaterials. 2012;33:4370-8.
48. Bonacchi S, Genovese D, Juris R, Montalti M, Prodi L, Rampazzo E, et al. Luminescent Chemosensors Based on Silica Nanoparticles. In: Prodi L, Montalti M, Zaccheroni N, editors.: Springer Berlin / Heidelberg; 2011. p. 93-138.
49. Kuo W-S, Chang Y-T, Cho K-C, Chiu K-C, Lien C-H, Yeh C-S, et al. Gold nanomaterials conjugated with indocyanine green for dual-modality photodynamic and photothermal therapy. Biomaterials. 2012;33(11):3270-8.
50. Pinho SLC, Faneca H, Geraldes CFGC, Delville M-H, Carlos LD, Rocha J. Lanthanide-DTPA grafted silica nanoparticles as bimodal-imaging contrast agents. Biomaterials. 2012;33(3):925-35.
51. Pinho SLC, Faneca H, Geraldes CFGC, Rocha J, Carlos LD, Delville M-H. Silica Nanoparticles for Bimodal MRI–Optical Imaging by Grafting Gd3+ and Eu3+/Tb3+ Complexes. European Journal of Inorganic Chemistry. 2012;2012(16):2828-37.
52. Altinoglu EI, Russin TJ, Kaiser JM, Barth BM, Eklund PC, Kester M, et al. Near-Infrared Emitting Fluorophore-Doped Calcium Phosphate Nanoparticles for In Vivo Imaging of Human Breast Cancer. ACS Nano. 2008;2(Copyright (C) 2012 American Chemical Society (ACS). All Rights Reserved.):2075-84.

53. Santra S, Liesenfeld B, Bertolino C, Dutta D, Cao Z, Tan W, et al. Fluorescence lifetime measurements to determine the core-shell nanostructure of FITC-doped silica nanoparticles: An optical approach to evaluate nanoparticle photostability. Journal of Luminescence. 2006;117(1):75-82.
54. Bagwe RP, Yang C, Hilliard LR, Tan W. Optimization of Dye-Doped Silica Nanoparticles Prepared Using a Reverse Microemulsion Method. Langmuir. 2004;20(19):8336-42.
55. Santra S, Tapec R, Theodoropoulou N, Dobson J, Hebard A, Tan W. Synthesis and Characterization of Silica-Coated Iron Oxide Nanoparticles in Microemulsion: The Effect of Nonionic Surfactants. Langmuir. 2001;17(10):2900-6.
56. Wang L, Wang K, Santra S, Zhao X, Hilliard LR, Smith JE, et al. Watching Silica Nanoparticles Glow in the Biological World. Analytical Chemistry. 2006;78(3):646-54.
57. Montalti M, Prodi L, Rampazzo E, Zaccheroni N. Dye-doped silica nanoparticles as luminescent organized systems for nanomedicine. Chemical Society Reviews. 2014;43(12):4243-68.
58. Vivero-Escoto JL, Huxford-Phillips RC, Lin W. Silica-based nanoprobes for biomedical imaging and theranostic applications. Chemical Society Reviews. 2012;41(7):2673-85.
59. Piao Y, Burns A, Kim J, Wiesner U, Hyeon T. Designed Fabrication of Silica-Based Nanostructured Particle Systems for Nanomedicine Applications. Advanced Functional Materials. 2008;18(23):3745-58.
60. Shirshahi V, Soltani M. Solid silica nanoparticles: applications in molecular imaging. Contrast Media & Molecular Imaging. 2015;10(1):1-17.
61. Hermanson GT. Chapter 14 - Microparticles and Nanoparticles. Bioconjugate Techniques (Third edition). Boston: Academic Press; 2013. p. 549-87.
62. Santra S, Zhang P, Wang K, Tapec R, Tan W. Conjugation of Biomolecules with Luminophore-Doped Silica Nanoparticles for Photostable Biomarkers. Analytical Chemistry. 2001;73(20):4988-93.
63. Larson DR, Ow H, Vishwasrao HD, Heikal AA, Wiesner U, Webb WW. Silica Nanoparticle Architecture Determines Radiative Properties of Encapsulated Fluorophores. Chemistry of Materials. 2008;20(8):2677-84.
64. Wolfbeis OS. An overview of nanoparticles commonly used in fluorescent bioimaging. Chemical Society Reviews. 2015;44(14):4743-68.
65. Energy Transfer. In: Lakowicz JR, editor. Principles of Fluorescence Spectroscopy. Boston, MA: Springer US; 2006. p. 443-75.
66. Stöber W, Fink A, Bohn E. Controlled growth of monodisperse silica spheres in the micron size range. Journal of Colloid and Interface Science. 1968;26(1):62-9.
67. Schmidt J, Guesdon C, Schomäcker R. Engineering Aspects of Preparation of Nanocrystalline Particles in Microemulsions. Journal of Nanoparticle Research. 1999;1(2):267-76.
68. Yong K-T, Roy I, Swihart MT, Prasad PN. Multifunctional nanoparticles as biocompatible targeted probes for human cancer diagnosis and therapy. Journal of Materials Chemistry. 2009;19(27):4655-72.
69. Alberto G, Caputo G, Viscardi G, Coluccia S, Martra G. Molecular Engineering of Hybrid Dye–Silica Fluorescent Nanoparticles: Influence of the Dye Structure on the Distribution of Fluorophores and Consequent Photoemission Brightness. Chemistry of Materials. 2012;24(14):2792-801.
70. Santra S, Wang K, Tapec R, Tan W. Development of novel dye-doped silica nanoparticles for biomarker application. BIOMEDO. 2001;6(2):160-6.
71. Zhao X, Tapec-Dytioco R, Tan W. Ultrasensitive DNA Detection Using Highly Fluorescent Bioconjugated Nanoparticles. Journal of the American Chemical Society. 2003;125(38):11474-5.
72. Tan W, Wang K, He X, Zhao XJ, Drake T, Wang L, et al. Bionanotechnology based on silica nanoparticles. Medicinal Research Reviews. 2004;24(5):621-38.

73. Tapec R, Zhao XJ, Tan W. Development of Organic Dye-Doped Silica Nanoparticles for Bioanalysis and Biosensors. Journal of Nanoscience and Nanotechnology. 2002;2(3-1):405-9.
74. Van Blaaderen A, Vrij A. Synthesis and characterization of colloidal dispersions of fluorescent, monodisperse silica spheres. Langmuir. 1992;8(12):2921-31.
75. Nyffenegger R, Quellet C, Ricka J. Synthesis of Fluorescent, Monodisperse, Colloidal Silica Particles. Journal of Colloid and Interface Science. 1993;159(1):150-7.
76. Verhaegh NAM, Blaaderen Av. Dispersions of Rhodamine-Labeled Silica Spheres: Synthesis, Characterization, and Fluorescence Confocal Scanning Laser Microscopy. Langmuir. 1994;10(5):1427-38.
77. Graf C, Schärtl W, Fischer K, Hugenberg N, Schmidt M. Dye-Labeled Poly(organosiloxane) Microgels with Core−Shell Architecture. Langmuir. 1999;15(19):6170-80.
78. Duguet E, Treguer-Delapierre M, Delville MH. Functionalised Inorganic Nanoparticles for Biomedical Applications. In: Boisseau P, Houdy P, Lahmani M, editors. Nanoscience: Springer Berlin Heidelberg; 2009. p. 129-70.
79. Ribot EJ, Miraux S, Konsman JP, Bouchaud V, Pourtau L, Delville M-H, et al. In vivo MR tracking of therapeutic microglia to a human glioma model. Nmr in Biomedicine. 2011;24(10):1361-8.
80. Voisin P, Ribot EJ, Miraux S, Bouzier-Sore A-K, Lahitte J-F, Bouchaud V, et al. Use of lanthanide-grafted inorganic nanoparticles as effective contrast agents for cellular uptake imaging. Bioconjugate Chemistry. 2007;18(4):1053-63.
81. Pinho SLC, Faneca H, Geraldes CFGC, Rocha J, Carlos LD, Delville M-H. Silica nanoparticles for bimodal MRI-optical imaging by grafting Gd3+ and Eu3+/Tb3+ complexes. Eur J Inorg Chem. 2012;2012(Copyright (C) 2014 American Chemical Society (ACS). All Rights Reserved.):2828-37.
82. Ow H, Larson DR, Srivastava M, Baird BA, Webb WW, Wiesner U. Bright and Stable Core−Shell Fluorescent Silica Nanoparticles. Nano Letters. 2005;5(1):113-7.
83. Burns A, Ow H, Wiesner U. Fluorescent core-shell silica nanoparticles: towards "Lab on a Particle" architectures for nanobiotechnology. Chemical Society Reviews. 2006;35(11):1028-42.
84. Phillips E, Penate-Medina O, Zanzonico PB, Carvajal RD, Mohan P, Ye Y, et al. Clinical translation of an ultrasmall inorganic optical-PET imaging nanoparticle probe. Science Translational Medicine. 2014;6(260):260ra149-260ra149.
85. Rampazzo E, Bonacchi S, Montalti M, Prodi L, Zaccheroni N. Self-Organizing Core−Shell Nanostructures: Spontaneous Accumulation of Dye in the Core of Doped Silica Nanoparticles. Journal of the American Chemical Society. 2007;129(46):14251-6.
86. Miletto I, Gilardino A, Zamburlin P, Dalmazzo S, Lovisolo D, Caputo G, et al. Highly bright and photostable cyanine dye-doped silica nanoparticles for optical imaging: Photophysical characterization and cell tests. Dyes and Pigments. 2010;84(1):121-7.
87. Alberto G, Miletto I, Viscardi G, Caputo G, Latterini L, Coluccia S, et al. Hybrid Cyanine−Silica Nanoparticles: Homogeneous Photoemission Behavior of Entrapped Fluorophores and Consequent High Brightness Enhancement. The Journal of Physical Chemistry C. 2009;113(50):21048-53.
88. Bonacchi S, Genovese D, Juris R, Montalti M, Prodi L, Rampazzo E, et al. Luminescent Silica Nanoparticles: Extending the Frontiers of Brightness. Angewandte Chemie International Edition. 2011;50(18):4056-66.
89. Hong Y, Lam JWY, Tang BZ. Aggregation-induced emission. Chemical Society Reviews. 2011;40(11):5361-88.
90. Yan L, Zhang Y, Xu B, Tian W. Fluorescent nanoparticles based on AIE fluorogens for bioimaging. Nanoscale. 2016;8(5):2471-87.
91. Wang X, Morales AR, Urakami T, Zhang L, Bondar MV, Komatsu M, et al. Folate Receptor-Targeted Aggregation-Enhanced Near-IR Emitting Silica Nanoprobe for One-Photon in

Vivo and Two-Photon ex Vivo Fluorescence Bioimaging. Bioconjugate Chemistry. 2011;22(7):1438-50.
92. Kim S, Pudavar HE, Bonoiu A, Prasad PN. Aggregation-Enhanced Fluorescence in Organically Modified Silica Nanoparticles: A Novel Approach toward High-Signal-Output Nanoprobes for Two-Photon Fluorescence Bioimaging. Advanced Materials. 2007;19(22):3791-5.
93. Kim S, Ohulchanskyy TY, Pudavar HE, Pandey RK, Prasad PN. Organically Modified Silica Nanoparticles Co-encapsulating Photosensitizing Drug and Aggregation-Enhanced Two-Photon Absorbing Fluorescent Dye Aggregates for Two-Photon Photodynamic Therapy. Journal of the American Chemical Society. 2007;129(9):2669-75.
94. Faisal M, Hong Y, Liu J, Yu Y, Lam JWY, Qin A, et al. Fabrication of Fluorescent Silica Nanoparticles Hybridized with AIE Luminogens and Exploration of Their Applications as Nanobiosensors in Intracellular Imaging. Chemistry – A European Journal. 2010;16(14):4266-72.
95. Mahtab F, Lam JWY, Yu Y, Liu J, Yuan W, Lu P, et al. Covalent Immobilization of Aggregation-Induced Emission Luminogens in Silica Nanoparticles Through Click Reaction. Small. 2011;7(10):1448-55.
96. Wang L, Tan W. Multicolor FRET Silica Nanoparticles by Single Wavelength Excitation. Nano Letters. 2006;6(1):84-8.
97. Xu J, Liang J, Li J, Yang W. Multicolor Dye-Doped Silica Nanoparticles Independent of FRET. Langmuir. 2010;26(20):15722-5.
98. Rosenholm JM, Sahlgren C, Linden M. Towards multifunctional, targeted drug delivery systems using mesoporous silica nanoparticles - opportunities & challenges. Nanoscale. 2010;2(10):1870-83.
99. Ambrogio MW, Thomas CR, Zhao Y-L, Zink JI, Stoddart JF. Mechanized Silica Nanoparticles: A New Frontier in Theranostic Nanomedicine. Accounts of Chemical Research. 2011;44(10):903-13.
100. Xie M, Shi H, Li Z, Shen H, Ma K, Li B, et al. A multifunctional mesoporous silica nanocomposite for targeted delivery, controlled release of doxorubicin and bioimaging. Colloids and Surfaces B-Biointerfaces. 2013;110:138-47.
101. Radu DR, Lai CY, Jeftinija K, Rowe EW, Jeftinija S, Lin VSY. A polyamidoamine dendrimer-capped mesoporous silica nanosphere-based gene transfection reagent. Journal of the American Chemical Society. 2004;126:13216-7.
102. Slowing II, Vivero-Escoto JL, Wu C-W, Lin VSY. Mesoporous silica nanoparticles as controlled release drug delivery and gene transfection carriers. Advanced Drug Delivery Reviews. 2008;60(11):1278-88.
103. Xia T, Kovochich M, Liong M, Meng H, Kabehie S, George S, et al. Polyethyleneimine Coating Enhances the Cellular Uptake of Mesoporous Silica Nanoparticles and Allows Safe Delivery of siRNA and DNA Constructs. Acs Nano. 2009;3(10):3273-86.
104. Meng H, Liong M, Xia T, Li Z, Ji Z, Zink JI, et al. Engineered Design of Mesoporous Silica Nanoparticles to Deliver Doxorubicin and P-Glycoprotein siRNA to Overcome Drug Resistance in a Cancer Cell Line. Acs Nano. 2010;4(8):4539-50.
105. Lu J, Liong M, Li ZX, Zink JI, Tamanoi F. Biocompatibility, Biodistribution, and Drug-Delivery Efficiency of Mesoporous Silica Nanoparticles for Cancer Therapy in Animals. Small. 2010;6(16):1794-805.
106. Tsai CP, Chen CY, Hung Y, Chang FH, Mou CY. Monoclonal antibody-functionalized mesoporous silica nanoparticles (MSN) for selective targeting breast cancer cells. Journal of Materials Chemistry. 2009;19(32):5737-43.
107. Cheng SH, Lee CH, Chen MC, Souris JS, Tseng FG, Yang CS, et al. Tri-functionalization of mesoporous silica nanoparticles for comprehensive cancer theranostics-the trio of imaging, targeting and therapy. Journal of Materials Chemistry. 2010;20(29):6149-57.

108. Zhang J, Yuan ZF, Wang Y, Chen WH, Luo GF, Cheng SX, et al. Multifunctional Envelope-Type Mesoporous Silica Nanoparticles for Tumor-Triggered Targeting Drug Delivery. Journal of the American Chemical Society. 2013;135(13):5068-73.
109. Meng H, Xue M, Zink JI, Nel AE. Development of Pharmaceutically Adapted Mesoporous Silica Nanoparticles Platform. Journal of Physical Chemistry Letters. 2012;3(3):358-9.
110. Rosenholm JM, Mamaeva V, Sahlgren C, Linden M. Nanoparticles in targeted cancer therapy: mesoporous silica nanoparticles entering preclinical development stage. Nanomedicine. 2012;7(1):111-20.
111. Sapino S, Ugazio E, Gastaldi L, Miletto I, G. B, Zonari D, et al. Mesoporous silica as topical nanocarriers for quercetin: characterization and in vitro studies. European Journal of Pharmaceutics and Biopharmaceutics. 2015;89:116–25.
112. Gignone A, Delle Piane M, Corno M, Ugliengo P, Onida B. Simulation and Experiment Reveal a Complex Scenario for the Adsorption of an Antifungal Drug in Ordered Mesoporous Silica. Journal of Physical Chemistry C. 2015;119(23):13068-79.
113. Gignone A, Manna L, Ronchetti S, Banchero M, Onida B. Incorporation of clotrimazole in Ordered Mesoporous Silica by supercritical CO2. Microporous and Mesoporous Materials. 2014;200:291-6.
114. Ugazio E, Gastaldi L, Brunella V, Scalarone D, Jadhav SA, Oliaro-Bosso S, et al. Thermoresponsive mesoporous silica nanoparticles as a carrier for skin delivery of quercetin. International Journal of Pharmaceutics. minor revisions.
115. Vallet-Regí M, Balas F, Arcos D. Mesoporous materials for drug delivery. Angewandte Chemie-International Edition. 2007;46:7548-58.
116. Ahmed N, Fessi H, Elaissari A. Theranostic applications of nanoparticles in cancer. Drug Discovery Today. 2012;17(17-18):928-34.
117. Wang Y, Cui Y, Huang J, Di D, Dong Y, Zhang X, et al. Redox and pH dual-responsive mesoporous silica nanoparticles for site-specific drug delivery. Applied Surface Science. 2015;356:1282-8.
118. DeMuth P, Hurley M, Wu CW, Galanie S, Zachariah MR, DeShong P. Mesoscale porous silica as drug delivery vehicles: Synthesis, characterization, and pH-sensitive release profiles. Microporous and Mesoporous Materials. 2011;141(1-3):128-34.
119. Guli M, Chen Y, Li X, Zhu G, Qiu S. Fluorescence of postgrafting Rhodamine B in the mesopores of rodlike SBA-15. Journal of Luminescence. 2007;126(2):723-7.
120. Lee CH, Lo LW, Mou CY, Yang CS. Synthesis and Characterization of Positive-Charge Functionalized Mesoporous Silica Nanoparticles for Oral Drug Delivery of an Anti-Inflammatory Drug. Advanced Functional Materials. 2008;18(20):3283-92.
121. Croissant JG, Zhang D, Alsaiari S, Lu J, Deng L, Tamanoi F, et al. Protein-gold clusters-capped mesoporous silica nanoparticles for high drug loading, autonomous gemcitabine/doxorubicin co-delivery, and in-vivo tumor imaging. Journal of Controlled Release. 2016;229:183-91.
122. Fan JQ, Fang G, Wang XD, Zeng F, Xiang YF, Wu SZ. Targeted anticancer prodrug with mesoporous silica nanoparticles as vehicles. Nanotechnology. 2011;22(45).
123. Kim H, Kim S, Park C, Lee H, Park HJ, Kim C. Glutathione-Induced Intracellular Release of Guests from Mesoporous Silica Nanocontainers with Cyclodextrin Gatekeepers. Advanced Materials. 2010;22(38):4280-+.
124. Sahoo B, Devi KSP, Dutta S, Maiti TK, Pramanik P, Dhara D. Biocompatible mesoporous silica-coated superparamagnetic manganese ferrite nanoparticles for targeted drug delivery and MR imaging applications. Journal of Colloid and Interface Science. 2014;431:31-41.
125. Nakamura T, Sugihara F, Matsushita H, Yoshioka Y, Mizukami S, Kikuchi K. Mesoporous silica nanoparticles for F-19 magnetic resonance imaging, fluorescence imaging, and drug delivery. Chemical Science. 2015;6(3):1986-90.

126. Yang G, Gong H, Qian X, Tan P, Li Z, Liu T, et al. Mesoporous silica nanorods intrinsically doped with photosensitizers as a multifunctional drug carrier for combination therapy of cancer. Nano Research. 2015;8(3):751-64.
127. Shao Y, Wang L, Zhang J, Anpo M. The photoluminescence of rhodamine B encapsulated in mesoporous Si-MCM-48, Ce-MCM-48, Fe-MCM-48 and Cr-MCM-48 molecular sieves. Journal of Photochemistry and Photobiology a-Chemistry. 2006;180(1-2):59-64.
128. Qu Y, Feng L, Liu B, Tong C, Lu C. A facile strategy for synthesis of nearly white light emitting mesoporous silica nanoparticles. Colloids and Surfaces a-Physicochemical and Engineering Aspects. 2014;441:565-71.
129. Wan XJ, Wang D, Liu SY. Fluorescent pH-Sensing Organic/Inorganic Hybrid Mesoporous Silica Nanoparticles with Tunable Redox-Responsive Release Capability. Langmuir. 2010;26(19):15574-9.
130. Hurley MT, Wang Z, Mahle A, Rabin D, Liu Q, English DS, et al. Synthesis, Characterization, and Application of Antibody Functionalized Fluorescent Silica Nanoparticles. Advanced Functional Materials. 2013;23(26):3335-43.
131. Martins Estevao B, Miletto I, Marchese L, Gianotti E. Optimized Rhodamine B labeled mesoporous silica nanoparticles as fluorescent scaffolds for the immobilization of photosensitizers: a theranostic platform for optical imaging and photodynamic therapy. Physical Chemistry Chemical Physics. 2016;18(13):9042-52.
132. Costanzo M, Carton F, Marengo A, Berlier G, Stella B, Arpicco S, et al. Fluorescence and electron microscopy to visualize the intracellular fate of nanoparticles for drug delivery. European Journal of Histochemistry. 2016;60(2):107-15.
133. Du P, Zhao X, Zeng J, Guo J, Liu P. Layer-by-layer engineering fluorescent polyelectrolyte coated mesoporous silica nanoparticles as pH-sensitive nanocarriers for controlled release. Applied Surface Science. 2015;345:90-8.
134. Morelli C, Maris P, Sisci D, Perrotta E, Brunelli E, Perrotta I, et al. PEG-templated mesoporous silica nanoparticles exclusively target cancer cells. Nanoscale. 2011;3(8):3198-207.
135. Chen YP, Chen HA, Hung Y, Chien FC, Chen PL, Mou CY. Surface charge effect in intracellular localization of mesoporous silica nanoparticles as probed by fluorescent ratiometric pH imaging. Rsc Advances. 2012;2(3):968-73.
136. Roggers RA, Lin VSY, Trewyn BG. Chemically Reducible Lipid Bilayer Coated Mesoporous Silica Nanoparticles Demonstrating Controlled Release and HeLa and Normal Mouse Liver Cell Biocompatibility and Cellular Internalization. Molecular Pharmaceutics. 2012;9(9):2770-7.
137. Nadrah P, Porta F, Planinsek O, Kros A, Gaberscek M. Poly(propylene imine) dendrimer caps on mesoporous silica nanoparticles for redox-responsive release: smaller is better. Physical Chemistry Chemical Physics. 2013;15(26):10740-8.
138. Qian R, Ding L, Ju H. Switchable Fluorescent Imaging of Intracellular Telomerase Activity Using Telomerase-Responsive Mesoporous Silica Nanoparticle. Journal of the American Chemical Society. 2013;135(36):13282-5.
139. Lai CY, Wu CW, Radu DR, Trewyn BG, Lin VSY. Reversible binding and fluorescence energy transfer between surface-derivatized CdS nanoparticles and multi-functionalized fluorescent mesoporous silica nanospheres. In: Xu R, Gao Z, Chen J, Yan W, editors. From Zeolites to Porous Mof Materials: The 40th Anniversary of International Zeolite Conference, Proceedings of the 15th International Zeolite Conference2007. p. 1827-35.
140. Martin-Ortigosa S, Valenstein JS, Lin VSY, Trewyn BG, Wang K. Gold Functionalized Mesoporous Silica Nanoparticle Mediated Protein and DNA Codelivery to Plant Cells Via the Biolistic Method. Advanced Functional Materials. 2012;22(17):3576-82.
141. Radu DR, Lai CY, Wiench JW, Pruski M, Lin VSY. Gatekeeping layer effect: A poly(lactic acid)-coated mesoporous silica nanosphere-based fluorescence probe for detection of amino-containing neurotransmitters. Journal of the American Chemical Society. 2004;126(6):1640-1.

142. Yang L, Li N, Pan W, Yu Z, Tang B. Real-Time Imaging of Mitochondrial Hydrogen Peroxide and pH Fluctuations in Living Cells Using a Fluorescent Nanosensor. Analytical Chemistry. 2015;87(7):3678-84.
143. Zhang D, Gao A, Xu Y, Yin X-B, He X-W, Zhang Y-K. Gd-Al co-doped mesoporous silica nanoparticles loaded with Ru(bpy)(3)(2+) as a dual-modality probe for fluorescence and magnetic resonance imaging. Analyst. 2014;139(18):4613-9.
144. Zeng C, Shang W, Wang K, Chi C, Jia X, Fang C, et al. Intraoperative Identification of Liver Cancer Microfoci Using a Targeted Near-Infrared Fluorescent Probe for Imaging-Guided Surgery. Scientific Reports. 2016;6.
145. Qu Y, Feng L, Tong C, Liu B, Lu C. Poly(p-phenylenevinylene) functionalized fluorescent mesoporous silica nanoparticles for drug release and cell imaging. Microporous and Mesoporous Materials. 2013;182:155-64.
146. Zhang X, Zhang X, Wang S, Liu M, Zhang Y, Tao L, et al. Facile Incorporation of Aggregation-Induced Emission Materials into Mesoporous Silica Nanoparticles for Intracellular Imaging and Cancer Therapy. Acs Applied Materials & Interfaces. 2013;5(6):1943-7.
147. Huang S, Song L, Xiao Z, Hu Y, Peng M, Li J, et al. Graphene quantum dot-decorated mesoporous silica nanoparticles for high aspirin loading capacity and its pH-triggered release. Analytical Methods. 2016;8(12):2561-7.
148. von Haartman E, Jiang H, Khomich AA, Zhang J, Burikov SA, Dolenko TA, et al. Core-shell designs of photoluminescent nanodiamonds with porous silica coatings for bioimaging and drug delivery I: fabrication. Journal of Materials Chemistry B. 2013;1(18):2358-66.
149. Prabhakar N, Nareoja T, von Haartman E, Sen Karaman D, Jiang H, Koho S, et al. Core-shell designs of photoluminescent nanodiamonds with porous silica coatings for bioimaging and drug delivery II: application. Nanoscale. 2013;5(9):3713-22.
150. Asefa T, MacLachlan MJ, Coombs N, Ozin GA. Periodic mesoporous organosilicas with organic groups inside the channel walls. Nature. 1999;402(6764):867-71.
151. Inagaki S, Guan S, Fukushima Y, Ohsuna T, Terasaki O. Novel mesoporous materials with a uniform distribution of organic groups and inorganic oxide in their frameworks. Journal of the American Chemical Society. 1999;121(41):9611-4.
152. Tani T, Mizoshita N, Inagaki S. Luminescent periodic mesoporous organosilicas. Journal of Materials Chemistry. 2009;19(26):4451-6.
153. Mizoshita N, Tani T, Inagaki S. Syntheses, properties and applications of periodic mesoporous organosilicas prepared from bridged organosilane precursors. Chemical Society Reviews. 2011;40(2):789-800.
154. Croissant JG, Cattoen X, Man MWC, Durand J-O, Khashab NM. Syntheses and applications of periodic mesoporous organosilica nanoparticles. Nanoscale. 2015;7(48):20318-34.
155. Guan B, Cui Y, Ren Z, Qiao Z-a, Wang L, Liu Y, et al. Highly ordered periodic mesoporous organosilica nanoparticles with controllable pore structures. Nanoscale. 2012;4(20):6588-96.
156. Goto Y, Mizoshita N, Ohtani O, Okada T, Shimada T, Tani T, et al. Synthesis of mesoporous aromatic silica thin films and their optical properties. Chemistry of Materials. 2008;20(13):4495-8.
157. Chandra D, Yokoi T, Tatsumi T, Bhaumik A. Highly luminescent organic-inorganic hybrid mesoporous silicas containing tunable chemosensor inside the pore wall. Chemistry of Materials. 2007;19(22):5347-54.
158. Du X, Li X, Xiong L, Zhang X, Kleitz F, Qiao SZ. Mesoporous silica nanoparticles with organo-bridged silsesquioxane framework as innovative platforms for bioimaging and therapeutic agent delivery. Biomaterials. 2016;91:90-127.
159. Lu D, Lei J, Wang L, Zhang J. Multifluorescently Traceable Nanoparticle by a Single-Wavelength Excitation with Color-Related Drug Release Performance. Journal of the American Chemical Society. 2012;134(21):8746-9.

160. Li D, Zhang Y, Fan Z, Chen J, Yu J. Coupling of chromophores with exactly opposite luminescence behaviours in mesostructured organosilicas for high-efficiency multicolour emission. Chemical Science. 2015;6(11):6097-101.
161. Corma A. State of the art and future challenges of zeolites as catalysts. Journal of Catalysis. 2003;216(1–2):298-312.
162. Corma A. From Microporous to Mesoporous Molecular Sieve Materials and Their Use in Catalysis. Chemical Reviews. 1997;97(6):2373-420.
163. Ruiz AZ, Brühwiler D, Dieu L-Q, Calzaferri G. Controlling Size and Morphology of Zeolite L. In: Schubert U, Hüsing N, Laine RM, editors. Materials Syntheses: A Practical Guide. Vienna: Springer Vienna; 2008. p. 9-19.
164. Wang Y, Li H. Luminescent materials of zeolite functionalized with lanthanides. CrystEngComm. 2014;16(42):9764-78.
165. Devaux A, Calzaferri G, Miletto I, Cao P, Belser P, Brühwiler D, et al. Self-Absorption and Luminescence Quantum Yields of Dye-Zeolite L Composites. The Journal of Physical Chemistry C. 2013;117(44):23034-47.
166. Cao P, Khorev O, Devaux A, Sägesser L, Kunzmann A, Ecker A, et al. Supramolecular Organization of Dye Molecules in ZeoliteL Channels: Synthesis, Properties, and Composite Materials. Chemistry - A European Journal. 2016.
167. Calzaferri G. Nanochannels: Hosts for the Supramolecular Organization of Molecules and Complexes. Langmuir. 2012;28(15):6216-31.
168. Devaux A, Calzaferri G, Belser P, Cao P, Brühwiler D, Kunzmann A. Efficient and robust host-guest antenna composite for light harvesting. Chemistry of Materials. 2014;26(23):6878-85.
169. Ruiz ZA, Brühwiler D, Ban T, Calzaferri G. Synthesis of Zeolite L. Tuning Size and Morphology. Monatshefte für Chemie / Chemical Monthly. 2005;136(1):77-89.
170. Ohsuna T, Slater B, Gao F, Yu J, Sakamoto Y, Zhu G, et al. Fine Structures of Zeolite-Linde-L (LTL): Surface Structures, Growth Unit and Defects. Chemistry – A European Journal. 2004;10(20):5031-40.
171. Li Z, Luppi G, Geiger A, Josel H-P, De Cola L. Bioconjugated Fluorescent Zeolite L Nanocrystals as Labels in Protein Microarrays. Small. 2011;7(22):3193-201.
172. Popović Z, Otter M, Calzaferri G, De Cola L. Self-Assembling Living Systems with Functional Nanomaterials. Angewandte Chemie International Edition. 2007;46(32):6188-91.
173. Huber S, Calzaferri G. Sequential Functionalization of the Channel Entrances of Zeolite L Crystals. Angewandte Chemie. 2004;116(48):6906-10.
174. Bossart O, Calzaferri G. Selfassembly of zeolite L crystals on biological self-cleaning surfaces. Microporous and Mesoporous Materials. 2008;109(1–3):392-7.
175. Megelski S, Lieb A, Pauchard M, Drechsler A, Glaus S, Debus C, et al. Orientation of Fluorescent Dyes in the Nano Channels of Zeolite L. The Journal of Physical Chemistry B. 2001;105(1):25-35.
176. Li H, Devaux A, Popović Z, Cola LD, Calzaferri G. Carboxyester functionalised dye–zeolite L host–guest materials. Microporous and Mesoporous Materials. 2006;95(1–3):112-7.

CAPTION TO FIGURES: